



An aza-nucleoside, fragment-like inhibitor of the DNA repair enzyme alkyladenine glycosylase (AAG)



Eduard Mas Claret^a, Balqees Al Yahyaee^a, Shuyu Chu^a, Ruan M. Elliott^b, Manuel Imperato^a, Arnaud Lopez^a, Lisiane B. Meira^c, Brendan J. Howlin^a, Daniel K. Whelligan^{a,*}

^a Department of Chemistry, University of Surrey, Guildford GU2 7XH, UK

^b Department of Nutritional Sciences, School of Biosciences and Medicine, University of Surrey, Guildford GU2 7XH, UK

^c Department of Clinical and Experimental Medicine, School of Biosciences and Medicine, University of Surrey, Guildford GU2 7XH, UK

ARTICLE INFO

Keywords:

Methylpurine DNA glycosylase (MPG)

Alkyladenine DNA glycosylase (AAG)

Base excision DNA repair

Ischaemic reperfusion

Small molecule inhibitor

Aza-nucleoside

ABSTRACT

The DNA repair enzyme AAG has been shown in mice to promote tissue necrosis in response to ischaemic reperfusion or treatment with alkylating agents. A chemical probe inhibitor is required for investigations of the biological mechanism causing this phenomenon and as a lead for drugs that are potentially protective against tissue damage from organ failure and transplantation, and alkylative chemotherapy. Herein, we describe the rationale behind the choice of arylmethylpyrrolidines as appropriate aza-nucleoside mimics for an inhibitor followed by their synthesis and the first use of a microplate-based assay for quantification of their inhibition of AAG. We finally report the discovery of an imidazol-4-ylmethylpyrrolidine as a fragment-sized, weak inhibitor of AAG.

1. Introduction

Alkyladenine glycosylase (AAG; also known as methylpurine DNA glycosylase, MPG, and alkyl-N-purine glycosylase, ANPG, EC: 3.2.2.21) is one of several DNA glycosylases that can initiate the base excision repair (BER) pathway by hydrolysis of a range of alkylated, oxidised or deaminated purine bases from the DNA backbone.¹ AAG's action generates apurinic (AP) sites, which are further processed by downstream BER enzymes. Despite its beneficial role, AAG overactivity on DNA lesions can lead to cellular necrosis and tissue damage. Specifically, AAG has been shown to drive alkylation-induced cytotoxicity in several mouse tissues, namely the cerebellum, spleen, thymus, bone marrow, pancreas and retina, with tissue damage reduced or absent in Aag-knockout mice and dramatically increased in Aag-overexpressing transgenic mice.^{2,3} Furthermore, in ischemia reperfusion mouse models, Aag-knockout mice display reduced tissue necrosis in liver, kidney and brain when compared to wild type.⁴ Ischemia reperfusion models mimic ischaemic stroke, liver and kidney failure, and organ transplantation. In these events the tissues are temporarily starved of their blood supply before sudden reperfusion results in a burst of reactive oxygen and nitrogen species (RONS). RONS can directly oxidise DNA bases but also lead to lipid peroxidation products, which alkylate DNA.⁵ Further to this, sterile inflammation is induced and the

recruitment of neutrophils and macrophages leads to further production of RONS.⁶ Both alkylation- and ischaemia reperfusion-induced AAG-dependent tissue necrosis is hypothesised to result from AAG activity on substantial numbers of alkylated and oxidised DNA bases leading to the accumulation of toxic repair intermediates in the DNA, which overwhelm the repair capacity of downstream BER enzymes.³ Stable, membrane-permeable inhibitors of AAG are required as chemical probes to further investigate these mechanisms and to form leads to potential chemoprotectives for patients on alkylative chemotherapy or to generate rapid treatments for minimising tissue damage from stroke, and organ failure and transplantation.

The only reported specific small molecule inhibitor of AAG is the natural polyphenolic flavonol morin, which was shown to act directly on AAG, and not through binding to DNA, with an IC₅₀ of 2.6 μM (measured using a gel-based biochemical assay).⁷ Although shown through surface plasmon resonance and control experiments to be specific for AAG and effective in cells, a myriad of other bioactivities have been reported for morin resulting from both its antioxidant activity and binding to biomacromolecules.^{8,9} These other bioactivities may confound results when used as a probe in biological studies. Therefore, we sought an alternative scaffold for chemical probe inhibitors through ligand-based design. Our specific requirements of a final probe molecule match those of the Structural Genomics

* Corresponding author.

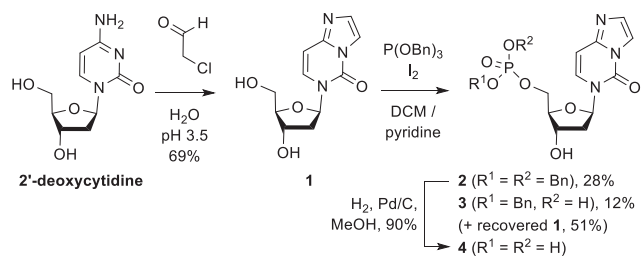
E-mail address: d.whelligan@surrey.ac.uk (D.K. Whelligan).

<https://doi.org/10.1016/j.bmc.2020.115507>

Received 10 February 2020; Received in revised form 6 April 2020; Accepted 9 April 2020

Available online 15 April 2020

0968-0896/ © 2020 Published by Elsevier Ltd.



Scheme 1. Synthesis of ethenodeoxycytidine **1** and 5'-phosphorylated analogues **2–4**.

Consortium for their Target 2035 program to make chemical or antibody probes available for the entire human proteome.^{10,11} Specifically, these are a biochemical assay K_d or $IC_{50} < 100$ nM, a cellular assay IC_{50} or $EC_{50} < 1$ μ M and > 30 -fold selectivity against other mammalian BER enzymes and enzymes known to be inhibited by structurally related molecules, such as purine nucleoside phosphorylase (PNP).

2. AAG small molecule inhibitor design

A duplex DNA 13-nucleotide oligomer containing an ethenodeoxycytidine (ϵ C) nucleotide is reported to inhibit AAG with an IC_{50} of 39 nM, and has a K_d of 21 nM.¹² This affinity is 2-fold greater than that of a 13-mer substrate ethenodeoxyadenosine (ϵ A)-containing oligomer ($K_d = 46$ nM). Based on this, we first sought to test the lone ϵ C-nucleoside **1** and nucleotide **4** (Scheme 1) for any inhibitory activity with a view to subsequently optimising them into potent, membrane permeable inhibitors if active. However, neither of these compounds, nor the precursor di- or mono- benzylphosphodiester **2** or **3** showed any inhibition at up to 1 mM concentration.

Another inhibitory duplex DNA oligomer, containing an abasic pyrrolidine (pyrr) nucleotide mimic (**pyrr-oligomer**, Fig. 1), was designed by the group of Verdine originally as an inhibitor of *Escherichia coli* 3-methyladenine DNA glycosylase II (AlkA).^{13,14} It is proposed that the protonated pyrrolidine mimics the oxocarbenium ion character of the transition state (TS) (or formal oxocarbenium intermediate in an S_N1 mechanism¹⁵), which involves cleavage of the *N*-glycosidic bond between the base and C-1' of the deoxyribose and attack by the nucleophilic active site water molecule from the opposite side.

In the published co-crystal structure (green, Fig. 1),¹³ the protonated pyrrolidine undergoes hydrogen bonding (2.8 Å) with the active site nucleophilic water molecule, which is itself held in place and activated by three hydrogen bonds with Glu125, Arg182 and the

backbone carbonyl of Val-262. Hydrogen bonding to this tightly bound water molecule is considered integral to the strong affinity ($K_d = 23$ pM) of this oligomer because the analogous uncharged tetrahydrofuran-containing oligomer showed $7 \times$ weaker binding ($K_d = 160$ pM).¹⁶ It is worthy of note that the pyrrolidine-containing oligomer is an effective inhibitor despite lacking a damaged DNA base mimic to occupy AAG's base-binding pocket.^{16,17} Nevertheless, a base mimic (adenine, joined to pyrrolidine via a CH_2 linker for stability) has been incorporated and a $K_d < 1$ pM against AAG reported.¹⁷ To the best of our knowledge, no X-ray crystal structure for this complex has been obtained and the lone nucleotide (or nucleoside) from this oligomer has not been tested against AAG.

To inform the design of small molecule inhibitors, we overlaid the published X-ray co-crystal structures of AAG in complex with the substrate ethenoadenine (ϵ A)-, inhibitory ϵ C- and pyrr-containing duplex oligomers (Fig. 1).¹⁸ [Note that the authors report that the ϵ A-oligomer remained un-hydrolysed in AAG's active site through use of inhibitory $MgCl_2$, Mg^{2+} ions from which were not seen in the crystal structure.] In the crystal structures, all of the DNA oligomers make several electrostatic/hydrogen bonding interactions between their phosphodiester groups and basic residues on the surface of AAG. Any potent small molecule inhibitor based on a single nucleotide would therefore have to find further binding interactions within the active site to compensate for the loss of the DNA chain (as exemplified by the lack of activity of our ϵ C lone nucleotides). Thus it would be necessary to include a base mimic to find interactions in AAG's base-binding pocket. To this end, we proposed to synthesise hybrid inhibitors based on the immucillin (discussed below) scaffolds containing the pyrrolidine moiety joined to an alkylated DNA-base analogue. This could be achieved in two ways:

1. in the form of inhibitor scaffold **5** where aromatic heterocycles are attached via a C-atom (to deprive them of leaving group ability) to C-1' position of the pyrrolidine, a design which takes account of the fact that in the overlay shown in Fig. 1, the ϵ C-deoxyribose (pink) overlaps well with the pyrrolidine group (green). Such molecules **5** are the subject of ongoing synthetic efforts in our group.
2. in the form of inhibitor scaffold **6** rationalised as follows: the overlay in Fig. 1 shows that, compared to the ϵ A-oligomer's deoxyribose group, the pyrrolidine is displaced towards the base-binding pocket. This could be to maximize hydrogen bonding with the nucleophilic water molecule or it could be due to the terminus of the ϵ A base pushing back against the end of its binding pocket. The latter is evidenced by the ϵ A-deoxyribose appearing displaced compared to the ϵ C-deoxyribose as well as the pyrrolidine. Either way, this

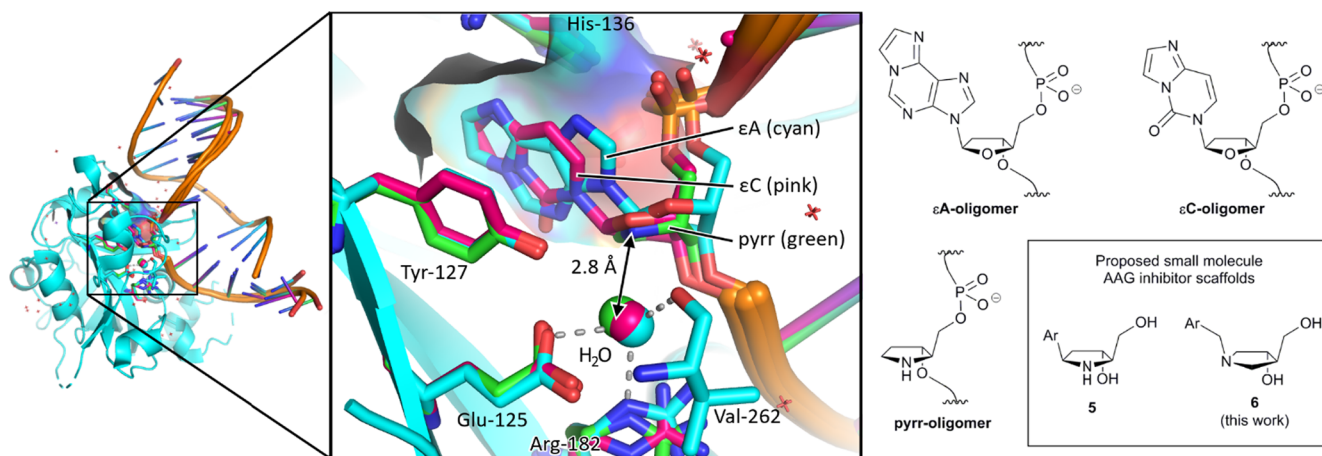


Fig. 1. Overlay of published X-ray co-crystal structures of AAG complexed with DNA oligomers containing: an (substrate) ethenodeoxyadenosine (ϵ A, cyan, PDB: 1F4R), an (inhibitory) ethenodeoxycytidine (ϵ C, pink, PDB: 3QI5) and an (inhibitory) abasic pyrrolidine nucleotide mimic (pyrr, green, PDB: 1F6O). The O-atoms of the overlaid, active site nucleophilic water molecules are coloured to match their crystal structures. Skeletal structures of the active-site bound nucleotides of these DNA oligomers are shown on the right along with small molecule inhibitor scaffolds proposed in this paper.

flexibility in the binding mode may permit the *N*-atom to be moved one position around the ring and itself to bear an alkylated base mimic, which must be linked via a CH₂ group to maintain the basicity (and therefore protonated form) of the pyrrolidine *N*-atom. Importantly, this positioning of the *N*-atom has been shown, in *Escherichia coli* 5'-methylthioadenosine/*S*-adenosylhomocysteine (MTAN), to better mimic a substrate transition state involving early, S_N1-like departure of the purine where most positive charge accumulates at the anomeric carbon.^{19,20} To the best of our knowledge, the “early-” or “late-ness” of the TS of AAG has not been determined and may be substrate specific for this multi-substrate enzyme. However, the comparison of both types of inhibitor in the future may inform on the nature of the TS to some extent.

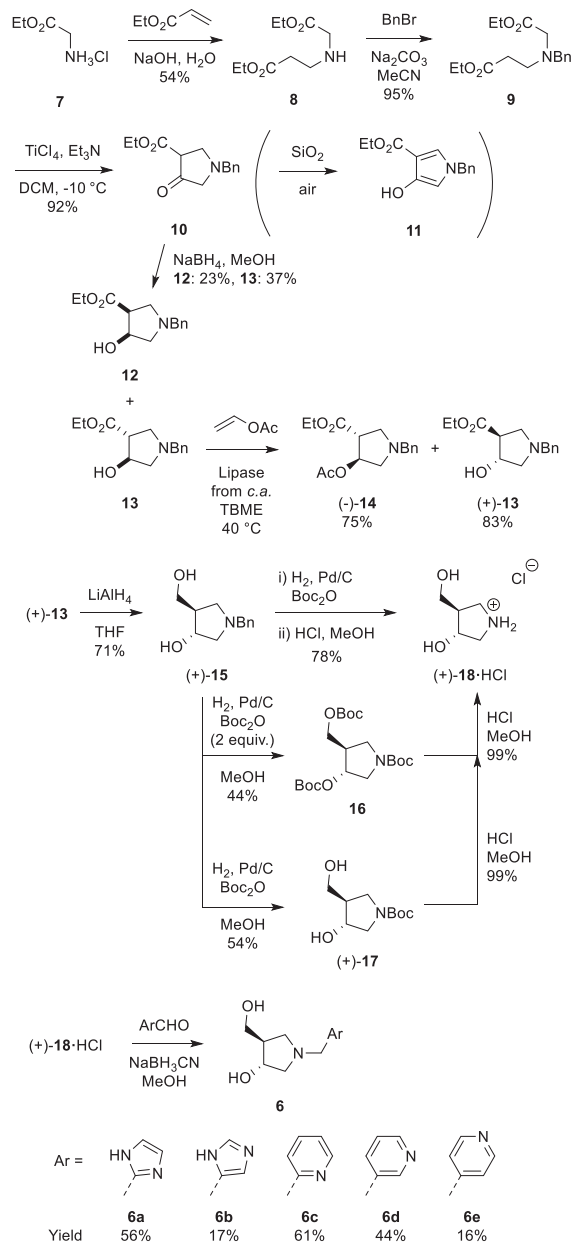
Both aza-nucleoside inhibitor scaffolds have been reported previously to mimic the transition states in enzymes which attack ribose- and deoxyribose-*N*-glycosidic bonds.²¹ For example, they form the first (5) and second (6) generation immucillins, which inhibit PNP by mimicking the TS of phosphorylation of guanosine and inosine.^{22–24} Also, compounds based on 6 inhibit the ADP-ribosylating action of the cholera, pertussis and diphtheria toxins,²⁵ and, as part of RNA-oligomers, the ricin A-chain.²⁶ Of most relevance to our work, the scaffolds have been previously applied as inhibitors of other DNA glycosylases, either as part of large DNA oligomers or as lone nucleosides. For example, a DNA 11-mer containing the abasic form (lacking any arylmethylene group) of nucleotide 6 showed a K_d of 0.11 nM against uracil DNA glycosylase (UDG),²⁷ and duplex DNA 30-mers containing nucleotides based on 5 and 6 are nano- to picomolar inhibitors of *Escherichia coli* MutY, bacterial Fpg, human 8-oxoguanine DNA glycosylase 1 (hOGG1) and human Nei-like DNA glycosylase (hNEIL1).^{28,29}

Herein, we report an investigation of the synthesis of five small molecule, free aza-nucleoside analogues based on scaffold 6 and the finding that one of them is a weak, but ligand efficient, inhibitor of AAG worthy of further optimisation into a chemical probe.

3. Chemistry

The free nucleoside and nucleotides of εC were synthesised from deoxycytidine as shown in Scheme 1. In our hands, ethenylation of 1 at RT required 7 days at pH 3.5 and complete removal of methanol and water from the purified product required extensive drying (100 °C under vacuum for 5 h) which may explain the higher m.p. obtained by us compared to others.³⁰ Conversion of nucleoside 1 into the phosphate was unsuccessful using POCl₃ with no product being isolable by reverse phase HPLC.³¹ To simplify purification, we opted for a dibenzylphosphorylation, which would permit normal phase chromatography of the protected phosphate prior to hydrogenolysis of the benzyl protecting groups. Thus, the tribenzylphosphite-iodine coupling^{32,33} was applied to afford a mixture of di- and mono-benzylphosphates 2 and 3 in low yield, along with recovery of starting material. To the best of our knowledge, this is the first application of that coupling to a nucleoside, albeit one bearing a non-nucleophilic base, and in a better-optimised form it may be a useful method for the selective phosphorylation of the primary alcohol of nucleosides without the need for secondary alcohol protection.³⁴ Subsequently, hydrogenation of dibenzylphosphate 2 afforded phosphite 4 in high yield, which was purified by reverse-phase HPLC prior to biochemical assay.

For the synthesis of azanucleosides 6, several routes to the key dihydroxypyrrolidine 18 (and its enantiomer) have been published, including those starting from sugars,^{35,36} those beginning with a 1,3-dipolar cycloaddition and later employing enzymatic chiral resolution,^{37–39} and those using an asymmetric 1,3-dipolar cycloaddition by means of chiral auxiliaries.^{40,41} Despite the latter two being 1–2 steps shorter, we chose to investigate the route based around the enzymatic chiral resolution of hydroxypyrrolidine 13 (Scheme 2), described by Clinch, and we report here some nuances of each reaction



Scheme 2. Synthesis of azanucleosides.

which may be of interest to the synthetic chemistry community.⁴² The route began with aza-Michael addition of glycine ethyl ester 7 to ethyl acrylate (1 equiv.) to give the corresponding secondary amine 8 in up to 54% yield.^{43,44} In several instances the tertiary amine resulting from a second aza-Michael addition of ethyl acrylate, was detected and removed by column chromatography. This has not been reported in the literature and it was not possible to prevent its formation by varying the rate of addition of ethyl acrylate or the reaction time. Subsequent *N*-benzylation of purified amine 8 afforded tertiary amine 9 in high yield.

The next step required a Dieckmann condensation to give pyrrolidinone 10. Pinto et al. showed that reaction of amine 9 with KOtBu in THF at –78 °C chemoselectively produced pyrrolidinone isomer 10 (74% yield) over the alternative isomer resulting from formation and attack by the enolate of the α-aminoester (13% yield).⁴⁵ In our case, formation of 10 was followed by GC–MS (*m/z* 247 [M⁺]) but, during chromatographic purification of the reaction mixture the desired product was oxidised to pyrrole 11 (characterised by GC–MS (*m/z* 245 [M⁺]) and NMR). The oxidation and aromatisation of oxo- and hydroxypyrrolidines to pyrroles in the presence of SiO₂ and air has been

reported by Davis et al.⁴⁶ A different purification procedure based on crystallisation of the product at $-4\text{ }^{\circ}\text{C}$ for 18 h was attempted, giving the desired pyrrolidine **10** in up to 60% yield, albeit with minor impurities. Due to the difficulties in purification of pyrrolidinone **10**, alternative, quantitative cyclisation conditions were sought to obviate the need for chromatography. The use of LDA gave a mixture of products and, again, only pyrrole **11** was isolated after chromatography. However, regioselective TiCl_4 -mediated Dieckmann condensation conditions, published by Deshmukh et al. and reported to give pyrrolidinone **10** and related compounds in 40–60% yield after chromatography,⁴⁷ proceeded in our hands to give 92% yield of **10** of sufficient purity to be used in the next step without purification, thus avoiding oxidation to the undesired pyrrole.

The next step involved borohydride reduction of pyrrolidinone **10**, using the conditions reported by Zhang et al., and gave a mixture of both β -hydroxyester diastereoisomers, in a $\sim 1:2$ ratio in favour of the desired *trans* form **13**, which was obtained in 37% yield after chromatography.⁴⁸ This is comparable to the literature yield on the identical substrate at large scale (42%)⁴⁹ but a lot lower than that reported for the reduction of the analogous *N*-Boc-protected (instead of Bn) pyrrolidinone (99%),⁴⁸ and could perhaps be improved in the future by use of the milder reducing agent NaBH_3CN .^{50,51}

Since fair amounts of the undesired *cis* diastereoisomer **12** were accumulated during this work, its epimerisation into the desired *trans* pyrrolidine **13** was studied on small scale (Table 1). Galeazzi et al. achieved quantitative epimerisation of an analogous compound using DBU in toluene at $70\text{ }^{\circ}\text{C}$ for 12 h but this was ineffective on pyrrolidine **12** (entry 1) and gave some eliminated alkene **19** along with eliminated and oxidised product pyrrole **20**.⁵³ The latter conversion **19** \rightarrow **20** has been previously described in dioxane at $90\text{ }^{\circ}\text{C}$.⁵² The alternative, weaker base Et_3N gave no reaction (entry 2) and use of $t\text{BuOK}$ gave more of, or mostly, the unsaturated products in toluene or THF (entries 3–5). A balance was found using EtONa in protic solvent EtOH which gave the desired diastereoisomer **13** as the largest component of the mixture (entry 6). Unfortunately, a single attempt at scale-up of this reaction gave none of the desired product, only an intractable mixture of highly polar compounds presumed to include ester hydrolysis products.

Enzymatic resolution of *trans*-pyrrolidine **13** was achieved according to Clinch et al. by enantioselective acylation catalysed by lipase B of *Candida antarctica* in *tert*-butyl methyl ether at $40\text{ }^{\circ}\text{C}$.⁴² After chromatographic separation, the desired hydroxypyrrolidine (+)-**13** was obtained in 83% yield with an $[\alpha]_{\text{D}}^{22}$ of $+19.5$, comparable to the literature value of $+16.9$. The acetylated form of the undesired enantiomer (–)-**14** was isolated in 75% yield with $[\alpha]_{\text{D}}^{22} = -40.7$, consistent with the literature value of -41.8 .

LiAlH_4 was used for the reduction of the ester moiety of (+)-**13** to

yield diol (+)-**15** in 71% yield. This was followed by *N*-debenzylation according to Clinch et al., who achieved quantitative yield for hydro-generation over Pd/C in the presence of di-*tert*-butyl dicarbonate to give the Boc-protected pyrrolidine (+)-**17** which is hydrolysed with HCl to give the pyrrolidine hydrochloride (+)-**18**-HCl.⁴² In our hands, this procedure gave unsatisfactory yields of *N*-Boc pyrrolidine (+)-**17** after purification, perhaps due to concurrent *O*-*tert*-butoxycarbonylation (*O*-Bocylation). In one instance, when more equivalents of Boc_2O were employed *N*-Boc-Bis-*O*-Boc-protected pyrrolidine **16** was isolated in 44% yield. Its characteristic features after ^1H NMR analysis were singlets at 1.49 ppm (18H) and 1.45 ppm (9H) corresponding to the three *tert*-butyl groups. The presence of three Boc groups was consistent with its ^{13}C NMR spectrum which showed three carbonyl signals at 153.9, 153.0 and 152.4 ppm. *O*-Bocylation, despite being rare compared to the analogous reaction on amines, has been reported in the literature for protection of alcohols using catalysts such as DMAP, zinc acetate, and perovskites (NaLaTiO_4).^{54–56}

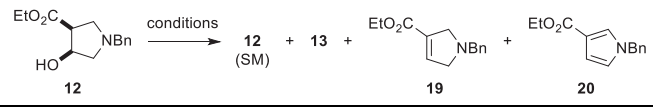
As both Boc-protected pyrrolidines could be successfully hydrolysed under the same conditions, a one-pot procedure was applied in later attempts to give (+)-**18**-HCl in a yield of up to 78%. The specific optical rotation measured for (+)-**18**-HCl ($[\alpha]_{\text{D}}^{21} = +16.0$) was in broad agreement with that found in the literature ($[\alpha]_{\text{D}}^{23} = +19.0$).⁴⁰

Finally, to access the proposed methylaryl inhibitors **6a–e**, reductive amination was applied to (+)-**18**-HCl and five heterocyclic aryl carbaldehydes. Initially, $\text{NaBH}(\text{OAc})_3$ was chosen as reducing agent due to its lower toxicity but this reagent requires the use of aprotic solvents (such as DCE and THF) in which the salt (+)-**18**-HCl was insoluble.⁵⁷ The alternative, but more toxic, reducing agent NaBH_3CN can be used in MeOH which effectively dissolved (+)-**18**-HCl and allowed the reaction to proceed.⁵⁸ No optimisation was carried out, but each small scale reaction provided sufficient quantity of the proposed inhibitors **6a–e** for biochemical testing against AAG.

4. Biochemical activity against AAG

The biochemical assay used to test inhibitor activity was based on the colorimetric microplate assay, previously reported by two of the authors, for determining base excision DNA repair enzyme activity.⁵⁹ Briefly, it involves surface-bound DNA containing a substrate residue for AAG (hypoxanthine) and terminal fluorescein. AAG's action leaves AP sites that render the DNA backbone prone to hydrolysis in the subsequent alkaline hydrolysis step, thus releasing the fluorescein-conjugated part of the DNA. The remaining 'plate-bound' fluorescein is detected using an anti-fluorescein antibody conjugated to horseradish peroxidase (HRP), incubation with a colour-changing substrate of HRP and colorimetric quantification. The assay was shown to be effective by testing published inhibitors ϵC -oligomer (lit. IC_{50} 39 nM, K_d 21 nM)¹²

Table 1
Epimerisation of *cis*-pyrrolidine **12** into *trans*-pyrrolidine **13**.



Entry	Base	Solvent	Temp/ $^{\circ}\text{C}$	Time /h	Product ratio by NMR ^a			
					12	13	19	20
1	DBU	Toluene	70	18	78	12	4	6
2	Et_3N	Toluene	70	17	100	0	0	0
3	$t\text{BuOK}$	Toluene	50	3	51	24	17	8
4	$t\text{BuOK}$	THF	50	2	trace	trace	62	38
5	$t\text{BuOK}$	THF	RT	17	0	0	75	25
6	EtONa	EtOH	RT	18	20	46	23	11

^a NMR peak integrals used to determine ratios: **12** (2.89 (1H, dd, J 10.0, 5.0 Hz, H-5a)); **13** (2.54 (1H, dd, J 9.5, 7.5 Hz, H-2b)); **19** (6.75 (1H, t, J H-4)); **20** (6.61, 6.62 (2H, 2 s, pyr-H) or 5.06 (1H, s, PhCH_2)).⁵² For example and reference spectra see ESI.

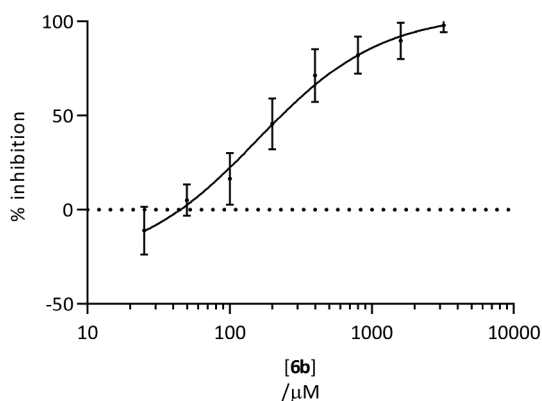


Fig. 2. IC_{50} curve of aza-nucleoside **6b** against AAG (0.05 U/ μ l). (U stands for enzyme unit, defined as the amount of enzyme which catalyses the conversion of 1 μ mol of substrate per minute.) Error bars show standard deviation of three replicates. Plotted using GraphPad Prism 7.04; curve fitted using equation: “[Inhibitor] vs. response”

and morin (lit. IC_{50} 2.6 μ M)⁷ which gave a comparable IC_{50} value of 21 nM for ϵ C-oligomer and a somewhat higher IC_{50} of 89 μ M for morin. The latter perhaps represents differences in the availability of morin under our conditions, particularly in terms of the buffer components used.

All five azanucleosides **6a–6e** were tested in this assay, which revealed that only **6b** exhibited detectable inhibitory activity (Fig. 2). Taking the mid-point between the top and bottom points of the curve, the IC_{50} of **6b** against AAG is 157 μ M. While this is weak activity against AAG, **6b** has a molecular weight of only 197 g mol⁻¹ and is comprised of only 14 ‘heavy’ (non-hydrogen) atoms, making it akin to a drug discovery fragment and,⁶⁰ leaving plenty of scope for increasing potency by the addition of further binding groups. In other words, **6b** shows a respectable, approximate (substituting IC_{50} for K_d) ligand efficiency of 0.37 kcal mol⁻¹ per heavy atom.⁶¹

5. Summary and conclusions

We have shown that the small molecule aza-nucleoside mimic **6b** possesses weak inhibitory activity against the DNA base excision repair enzyme AAG. Owing to its low molecular weight, **6b** is a ligand-efficient starting point for future optimisation into a more potent, selective and membrane-permeable AAG inhibitor. This is in contrast to nucleoside ethenodeoxycytidine **1** (and 5'-phosphates thereof), which we have shown to exhibit no inhibition outside of a DNA oligomer. IC_{50} of these small molecules was determined using our microplate-based colorimetric assay as opposed to the more involved but established radiolabel, gel-based assay.

In order to synthesise **6b** and its aryl analogues, we made a detailed study of one of the routes, largely reported by Clinch et al., and discovered several nuances of the chemistry including: 1. improved access to pyrrolidinone **10** using a $TiCl_4$ -mediated cyclisation which negated the need for column chromatography which otherwise led to oxidation to the pyrrole; 2. Isolation of the *cis* hydroxy-ester **12**, as well as the desired *trans* **13**, from reduction of the pyrrolidinone **10**, and the possibility (on small scale) of its conversion to the *trans* using sodium ethoxide; 3. Concurrent *O*-bocylation (along with desired *N*-bocylation) of pyrrolidine-diol **15** during hydrogenative removal of the *N*-benzyl group in the presence of excess Boc_2O ; and, 4. The requirement to use $NaBH_3CN$, rather than $NaBH(OAc)_3$, for reductive amination of pyrrolidinium salt **18.HCl** due to its compatibility with MeOH, the solvent required for dissolution of **18.HCl**. In addition, during synthesis of ethenocytidine phosphate, it was found that a tribenzylphosphite-iodine coupling of ethenocytidine, previously never applied to nucleosides, followed by hydrogenation, gave selectively the desired 5'-phosphate.

6. Experimental

6.1. General

Where used, solvents specified as “dry” were made so by being passed through activated alumina columns, using a Pure Solv™ Micro Solvent Purification System, and were stored over activated molecular sieves (3 Å, 8 to 12 mesh).⁶² Flash column silica chromatography was carried out using silica gel 40-63u 60 Å. Analytical thin layer chromatography (TLC) was performed using pre-coated aluminium-backed plates (silica gel 60 F254) and visualised by UV radiation at 254 nm, and/or by staining with basic potassium permanganate solution (K_2CO_3 (13.3 g), $KMnO_4$ (2 g), water (200 mL), NaOH solution (10% w/v, 1.7 mL)). HPLC purity was assessed (compounds **1–4** only) on a Varian 920-LC Liquid Chromatography system and the conditions were as follows: inj. vol. 20 μ L, column Varian Pursuit XRs 5 μ C18 (150 mm \times 4.6 mm), column temp. 40 °C, flow rate: 1 mL min⁻¹, mobile phase (compounds **1–3**) Solvent A, water, Solvent B, MeOH, mobile phase (compound **4**) Solvent A, water (0.1% formic acid), Solvent B, MeOH (0.1% formic acid), gradient 0–10 min, 10–90% B; 10–15 min, 90% B; 15–17 min, 90–10% B; 17–20 min, 10% B, detection: UV 254 nm. Infra-red (IR) spectra were recorded in the range 600–4000 cm⁻¹ using an Agilent Clary 600 FTIR spectrometer with MKII Golden Gate Single Reflection ATR System. NMR spectra were obtained on Bruker 500 MHz, 400 MHz or 300 MHz spectrometers. ¹H NMR spectra were referenced either to TMS at 0 ppm or to residual (partially) protic solvent: 3.31 ppm for CHD_2OD , 4.79 ppm for DOH or 7.26 ppm for $CHCl_3$. The data is given as follows: chemical shift (δ) in ppm, integration, multiplicity, coupling constants *J* (Hz), assignment (where given, for non-trivial compounds, assignment was made using DEPT, COSY, HSQC, HMBC and/or NOESY – see ESI – or by comparison with literature in which assignments were made). ¹³C NMR spectra were recorded at 126 MHz, 101 MHz or 75 MHz. They were referenced to $CDCl_3$ at 77.0 ppm or CD_3OD at 49.0 ppm. ³¹P NMR were recorded at 202 MHz. The data is given as follows: chemical shift (δ) in ppm, assignment. All chemical shifts are expressed as parts per million relative to tetramethylsilane ($\delta_H = 0.00$ ppm) and coupling constants are given in Hertz to the nearest 0.5 Hz. GC–MS spectra were recorded on an Agilent Technologies 7890A GC system connected to an Agilent Technologies 5975C inert XL EI/CI mass selective detector (MSD) operating in electron impact (EI) mode and the conditions were as follows: inj. vol. 1 μ L, inj. temp. 250 °C, column Agilent HP-5MS (30 m \times 0.25 mm), carrier gas (He) flow 1 mL min⁻¹, oven temperature gradient 0–3 min, 50 °C; 3–23 min, 50–250 °C (10 °C ramp per minute), 23–25 min, 250 °C. HRMS spectra were recorded using either a Waters QTOF Premier using electrospray ionisation (compounds **1–4**) or an Agilent 1260 Infinity II coupled to an Agilent 6550 iFunnel QTOF mass spectrometer using electrospray ionisation (remaining compounds). LC conditions for the latter were as follows: inj. vol. 1.00 μ L, column Agilent Extend-C18, column temp. 30 °C, flow rate 1.0 mL min⁻¹, mobile phase Solvent A: water (0.1% formic acid), Solvent B: MeCN (0.1% formic acid), gradient 0–3 min, 5–100% B; 3–3.5 min, 100% B; 3.5–4 min, 5% B. Specific optical rotation was recorded using a Jasco P-2000 Polarimeter; concentration of the sample (*c*) is given in g/100 mL.

6.2. 3,4'-Etheno-2'-deoxycytidine (5,6-Dihydro-5-oxo-6-(β -D-2'-deoxyribofuranosyl)imidazo[1,2-c]pyrimidine) (1)

A solution of 2'-deoxycytidine (0.10 g, 0.44 mmol) was dissolved in 50% w/w aqueous chloroacetaldehyde (1.1 mL, 8.8 mmol). The solution was adjusted to pH 3.5 by adding 1 M KOH aqueous solution and stirred at room temperature for 7 days during which time the solution was kept at pH 3.5. The reaction mixture was evaporated and purified by flash column chromatography (MeOH in DCM 5–15%). After evaporation of the fractions, a white solid form was obtained which was dissolved in a small amount of ethanol and precipitated by slowly

adding petroleum ether under ultrasound. The precipitate was filtered and dried at 100 °C under vacuum for 5 h to give the title compound as a white powder (76 mg, 69%); m.p. 149–151 °C (lit. 137–138 °C); purity 99.6% by HPLC; IR ν_{\max} (cm⁻¹) 3456 (O–H), 3112 (Ar–H), 1657 (C=O); ¹H NMR (500 MHz, DMSO-*d*₆) δ 7.80 (1H, s, H-2), 7.74 (1H, d, *J* 8.0 Hz, H-7), 7.40 (1H, s, H-3), 6.73 (1H, d, *J* 8.0 Hz, H-8), 6.42 (1H, t, *J* 7.0 Hz, H-1'), 5.32 (1H, m, 3'-OH), 5.09 (1H, m, 5'-OH), 4.30 (1H, m, H-4'), 3.86 (1H, m, H-3'), 3.61 (2H, m, H-5'), 2.23 (2H, m, H-2'); ¹³C NMR (126 MHz, DMSO-*d*₆) δ 145.9, 144.1, 133.0, 128.4, 113.2, 99.0, 88.2, 85.7, 70.8, 61.7, 40.6; HRMS (ESI) *m/z* calcd for C₁₁H₁₃N₃O₄Na [M + Na]⁺ 274.0803, found 274.0794; [α]_D²⁰ = +42.8 (c 2.0, MeOH); NMR data agrees with that given in the literature.^{30,63}

6.3. 3,*N*⁴-Etheno-2'-deoxycytidine-5'-(dibenzyl)phosphate (6-(5'-O-(dibenzyl)phosphate- β -D-2'-deoxyribofuranosyl)-5,6-dihydroimidazo[1,2-*c*]pyrimidin-5-one) (2)

Iodine (0.15 g, 0.60 mmol) was added to a solution of tribenzylphosphite (0.26 g, 0.72 mmol), prepared according to Wong et al.⁶⁴ in dry DCM (3.0 mL) with stirring at –20 °C. A colourless solution was obtained after iodine had dissolved and was slowly added to a solution of ethenocytidine (0.15 g, 0.60 mmol) in dry pyridine (3.0 mL) with stirring at –20 °C to give a pale brown solution. The reaction mixture was stirred for 2 h at RT, then quenched by adding one drop of water. After evaporation of solvent, a yellowish oil was obtained which was subjected to flash column chromatography (MeOH in DCM 2–35%) to give the title compound as a colourless oil (87 mg, 28%); R_f (DCM/MeOH 10:1) 0.48; purity 96.6% by HPLC; IR ν_{\max} (cm⁻¹) 1701 (C=O), 1627 (C=N), 1268 (C–O), 993; ¹H NMR (500 MHz, CDCl₃) δ 7.68 (1H, s), 7.35–7.16 (12H, m), 6.49 (1H, t, *J* 6.6 Hz), 6.43 (1H, d, *J* 7.8 Hz), 5.02 (4H, m), 4.41 (1H, m), 4.20 (2H, m), 4.07 (1H, m), 2.44 (1H, m), 2.10 (1H, m); ¹³C NMR (126 MHz, CDCl₃) δ 145.7, 144.9, 135.3 (d, ³J_{P-C} 6.5 Hz), 132.6, 128.9, 128.8, 128.7, 128.2, 128.1, 126.7, 112.8, 99.4, 85.7, 84.9 (d, ³J_{P-C} 7.6), 70.6, 69.9 (d, ²J_{P-C} 4.9), 69.8 (d, ²J_{P-C} 4.9), 66.7 (d, ²J_{P-C} 5.3), 40.5; ³¹P NMR (202 MHz, CDCl₃) δ –0.52 (m); HRMS (ESI) *m/z* calcd for C₂₅H₂₇N₃O₇P [M + H]⁺ 512.1586, found 512.1562; [α]_D²⁰ = +31.1° (c 0.8, MeOH).

6.4. (6-(5'-O-(monobenzyl)phosphate- β -D-2'-deoxyribofuranosyl)-5,6-dihydroimidazo[1,2-*c*]pyrimidin-5-one) (3)

Further elution of the column described gave monobenzyl phosphate **3** which was further purified by reverse-phase HPLC (MeOH in 0.1% aqueous HCO₂H 20–80%) to give a white solid (31 mg, 12%); m.p. 122–124 °C; R_f (DCM/MeOH 10:1) 0.08; purity 99.8% by HPLC; IR ν_{\max} (cm⁻¹) 1721 (C=O), 1630 (C=N), 997; ¹H NMR (500 MHz, D₂O) δ 8.15 (1H, d, *J* 7.9 Hz), 7.98 (1H, d, *J* 2.0 Hz), 7.72 (1H, d, *J* 2.0 Hz), 7.35–7.26 (10H, m), 6.89 (1H, d, *J* 7.9 Hz), 6.42 (1H, t, *J* 6.5 Hz), 4.90 (2H, m), 4.41 (1H, m), 4.23 (1H, m), 4.11 (1H, m), 4.02 (1H, m) 2.55 (1H, m), 2.30 (1H, m); ¹³C NMR (126 MHz, D₂O) δ 144.6, 143.9, 137.8 (d, ³J_{P-C} 6.7 Hz), 136.8, 129.1, 128.6, 128.0, 122.3, 114.5, 93.4, 88.5, 87.1 (d ³J_{P-C} 9.0 Hz), 71.3, 68.2 (d, ²J_{P-C} 5.5 Hz), 65.4 (d, ²J_{P-C} 5.1 Hz), 40.5; ³¹P NMR [202 MHz, D₂O] δ 0.27 (m); HRMS (ESI) *m/z* calcd for C₁₈H₁₉N₃O₇P [M – H][–] 420.0961, found 420.0956; [α]_D²⁰ = +46.9 (c 1.7, H₂O).

Further elution of the silica flash column gave recovered starting material **1** (76 mg, 51%).

6.5. 3,*N*⁴-Etheno-2'-deoxycytidine-5'-phosphate ((6-(5'-O-phosphate- β -D-2'-deoxyribofuranosyl)-5,6-dihydroimidazo[1,2-*c*]pyrimidin-5-one) (4)

Pd/C (18 mg 10% (w/w) containing 50% H₂O) was added to a solution of dibenzylphosphate **2** (30 mg, 0.05 mmol) in methanol (5 mL). The atmosphere was replaced with H₂ (balloon) and the reaction mixture was stirred 1 h. The mixture was filtered through Celite® and washed with methanol (15 mL). The colourless filtrate was

concentrated and purified by reverse-phase column chromatography (Biotage® SNAP KP-C18-HS cartridge, MeOH/H₂O 10–80%). After evaporation of methanol under reduced pressure, the aqueous solution was freeze-dried to give the title compound as a white powder (18 mg, 90%); purity 98.6% by HPLC; mp 142–144 °C (dec.); IR ν_{\max} (cm⁻¹) 3104 (Ar–H), 2942, 1720 (C=O), 1630 (C=N), 930, 738; ¹H NMR (500 MHz, D₂O) δ 8.32 (1H, d, *J* 8.0 Hz), 8.04 (1H, d, *J* 2.1 Hz), 7.75 (1H, d, *J* 2.1 Hz), 7.07 (1H, d, *J* 8.0 Hz), 6.51 (1H, t, *J* 6.5), 4.61 (1H, m), 4.31 (1H, m), 4.14 (2H, m), 2.61 (1H, m), 2.44 (1H, m); ¹³C NMR (126 MHz, D₂O) δ 144.9, 144.1, 137.0, 122.2, 114.5, 93.6, 88.4, 87.2 (d, ³J_{P-C} 8.6), 71.3, 65.0 (d, ²J_{P-C} 4.8 Hz), 40.6; ³¹P NMR (202 MHz, D₂O) δ –0.01; HRMS (ESI) *m/z*: [M][–] 330.0502, calc. 330.0491; [α]_D²⁰ = +66.3 (c = 0.8, H₂O).

6.6. 3-[N-(Carboxymethyl)amino]propanoic acid bis(ethyl ester) (8)

To a solution of NaOH (2.00 g, 50 mmol) in water (21 mL) was added glycine ethyl ester hydrochloride **7** (6.73 g, 50 mmol). The mixture was cooled to 0 °C under N₂ and ethyl acrylate (5.3 mL, 50 mmol) was added dropwise. The mixture was allowed to warm to RT and stirred vigorously for 15 h.⁴³ The reaction mixture was extracted with DCM (3 × 20 mL). The combined organic layers were washed with brine (2 × 20 mL), dried over anhydrous MgSO₄, filtered, concentrated and dried *in vacuo*. Flash column silica chromatography (DCM/EtOAc [1:2]) gave the title compound as a colourless oil (5.29 g, 54%); R_f (DCM/EtOAc [1:2]) 0.20; IR ν (cm⁻¹) 3338 (N–H), 2982, 1730 (C=O), 1617, 1439, 1372, 1254, 1178 (C–O), 1096, 1026; NMR δ_{H} (300 MHz; CDCl₃) 4.19 (2H, q, *J* 7.0 Hz, CH₂CH₃), 4.15 (2H, q, *J* 7.0 Hz, CH₂CH₃), 3.41 (2H, s, NHCH₂CO), 2.90 (2H, t, *J* 6.5 Hz, H-3), 2.51 (2H, t, *J* 6.5 Hz, H-2), 1.82 (1H, bs, H-1), 1.28 (3H, t, *J* 7.0 Hz, CH₂CH₃), 1.26 (3H, t, *J* 7.0 Hz, CH₂CH₃); δ_{C} (75 MHz; CDCl₃) 172.4 (CO), 172.2 (CO), 60.8 (CH₂CH₃), 60.5 (CH₂CH₃), 50.9 (NHCH₂CO), 44.8 (C-3), 34.9 (C-2), 14.2 (CH₂CH₃), 14.2 (CH₂CH₃); GC–MS t_R = 14.0 min, *m/z* (EI) 203 (M⁺, 11%), 157 (12%), 131 (19%), 130 (100%), 116 (100%), 84 (100%), 57 (10%), 56 (16%); ¹H NMR and IR data agree with those published in the literature.⁶⁵

6.7. 3-(benzyl-ethoxy-carbonylmethyl-amino)-propionic acid ethyl ester (9)

A mixture of **8** (4.767 g, 23.47 mmol) and NaHCO₃ (2.225 g, 26.52 mmol) were dissolved in dry acetonitrile (26 mL). The system was flushed with N₂ and benzyl bromide (2.8 mL, 23.47 mmol) was added dropwise while stirring. The reaction mixture was stirred under N₂ for 16 h.⁴³ The reaction was quenched using water (40 mL) and extracted with DCM (3 × 40 mL). The organic layer was washed with water (100 mL), brine (2 × 100 mL), dried over anhydrous MgSO₄, filtered, concentrated and dried *in vacuo*. Flash column silica chromatography of the resulting crude mixture (Pet. ether/EtOAc [9:1]) gave the title compound as a clear oil (6.56 g, 95%); R_f (Pet. ether/EtOAc [9:1]) 0.33; IR ν (cm⁻¹) 2981, 2852, 1730 (C=O), 1453, 1370, 1247, 1181 (C–O), 1144, 1027; NMR δ_{H} (300 MHz; CDCl₃) 7.34–7.21 (5H, m, Ph), 4.15 (2H, q, *J* 7.0 Hz, CH₂CH₃), 4.13 (2H, q, *J* 7.0 Hz, CH₂CH₃), 3.82 (2H, s, PhCH₂), 3.33 (2H, s, NCH₂CO), 3.05 (2H, t, *J* 7.0 Hz, H-3), 2.49 (2H, t, *J* 7.0 Hz, H-2), 1.26 (3H, t, *J* 7.0 Hz, CH₂CH₃), 1.24 (3H, t, *J* 7.0 Hz, CH₂CH₃); δ_{C} (126 MHz, CDCl₃) 172.5 (CO), 171.3 (CO), 138.8 (Ph), 128.8 (Ph), 128.3 (Ph), 127.2 (Ph), 60.4 (CH₂CH₃), 60.3 (CH₂CH₃), 57.8 (PhCH₂), 53.9 (NCH₂CO), 49.7 (C-3), 33.6 (C-2), 14.3 (CH₂CH₃), 14.2 (CH₂CH₃); GC–MS t_R = 20.4 min. *m/z* (EI) 293 (M⁺, 1%), 221 (16%), 220 ([M – COOEt]⁺, 100%), 206 (35%), 202 (10%), 91 (PhCH₂⁺, 100%). Literature IR data (from the year 1965) does not match.⁴⁹

6.8. Ethyl 1-benzyl-4-oxopyrrolidine-3-carboxylate (10)

To a solution of 1 M TiCl₄ in dry DCM (3.43 mL) at –10 °C was

added diester **9** (1.00 g, 3.41 mmol) in dry DCM (20 mL) and the resulting mixture was stirred at $-10\text{ }^{\circ}\text{C}$ for 0.5 h. Et_3N (1.1 mL, 7.51 mmol) was added dropwise slowly and the mixture was stirred for 2.5 h.⁴⁷ The reaction mixture was poured into saturated NaCl solution (25 mL) and the pH was made basic (~ 8) with Et_3N while stirring. The precipitated salts were filtered through Celite® and washed with DCM. After extraction with DCM ($3 \times 25\text{ mL}$), the combined organic layers were washed using saturated NaHCO_3 solution ($5 \times 75\text{ mL}$), dried over anhydrous MgSO_4 , filtered, concentrated and dried *in vacuo*. The crude material, a yellow oil, was used directly in the following step (0.77 g, 92%); R_f (Pet. ether/EtOAc [9:1]) 0.2; IR ν (cm^{-1}) 2981, 2806, 1767 (C=O), 1725 (C=O), 1028 (C–O); NMR δ_{H} (500 MHz; CDCl_3): 7.39–7.23 (5H, m, Ph), 4.24 (2H, qd, J 7.0, 1.0 Hz, OCH_2CH_3), 3.77 (1H, d, J 13.0 Hz, PhCHH-), 3.72 (1H, d, J 13.0 Hz, PhCHH-), 3.46 (1H, t, J 8.5 Hz, H-2a), 3.35 (1H, t, J 9.5 Hz, H-3), 3.27 (1H, d, J 17.0 Hz, H-5a), 3.09 (1H, t, J 9.0 Hz, H-2b), 2.91 (1H, d, J 17.0 Hz, H-5b), 1.29 (3H, t, J 7.0 Hz, OCH_2CH_3); δ_{C} (101 MHz, CDCl_3): 206.5 (CO), 167.4 (COOEt), 137.1 (Ph), 128.7 (Ph), 128.5 (Ph), 127.6 (Ph), 61.7 (OCH_2CH_3), 61.1 (C-5), 60.2 (PhCH₂), 54.7 (C-3), 54.2 (C-2), 14.2 (CH_3CH_2). GC–MS t_{R} = 18.8 min. m/z (EI) 247 (M^+ , 2%), 174.1 ($[\text{M} - \text{COOEt}]^+$, 65%), 117 (4%), 91 (100%), 65 (7%). No literature data for this (ethyl diester) compound is available.⁴²

6.9. 1-benzyl-4-hydroxy-1H-pyrrole-3-carboxylate (11)

Flash column silica chromatography of a sample of ketone **10** in air (Pet. Ether/AcOEt [9:1]) and secondly (DCM/Pet. Ether [3:1]) gave the title compound as a colourless oil; R_f 0.45; NMR δ_{H} (400 MHz; CDCl_3) 7.32–7.23 (3H, m, Ph), 7.03 (2H, d, J 7.5 Hz, Ph), 6.66 (1H, d, J 3.0 Hz, 5-H), 5.83 (1H, d, J 3.0 Hz, 2-H), 5.30 (2H, s, PhCH₂), 4.25 (2H, q, J 7.0 Hz, CH_3CH_2), 1.55 (1H, bs, OH), 1.22 (3H, t, J 7.0 Hz, CH_3CH_2); GC–MS t_{R} = 20.2 min m/z (EI) 245 (M^+ , 49%), 200 (11%), 199 (35%), 198 (28%), 91 (PhCH₂⁺, 100%); 1H NMR data is comparable to the limited peaks reported in the literature.⁶⁶

6.10. Ethyl *rel*-(3R,4R)-1-benzyl-4-hydroxypyrrolidine-3-carboxylate ((±)-12)

To a solution of oxopyrrolidine **7** (2.480 g, 10.03 mmol) in dry degassed MeOH (20 mL) at $0\text{ }^{\circ}\text{C}$ was added slowly NaBH_4 (0.190 g, 5.01 mmol).⁴⁸ The mixture was stirred for 2 h at $0\text{ }^{\circ}\text{C}$. After this time, GC–MS analysis revealed that starting oxopyrrolidine was still present, so 0.5 extra eq. of NaBH_4 (0.190 g, 5.01 mmol) were added at $0\text{ }^{\circ}\text{C}$ and the mixture was allowed to warm to RT and stirred overnight. After removal of solvents *in vacuo*, the residue was dissolved in water and extracted with DCM/MeOH 9:1 ($6 \times 20\text{ mL}$). The combined organic layers were washed with brine ($2 \times 60\text{ mL}$), dried over anhydrous MgSO_4 , filtered, concentrated and dried *in vacuo*. Flash column silica chromatography (Pet. Ether/EtOAc [4:1], 1% Et_3N to Pet. Ether/EtOAc [1:1], 1% Et_3N) gave first the *cis* isomer (±)-**12** as a yellow oil (0.57 g, 23%); R_f (Pet. Ether/EtOAc [1:1], 1% Et_3N) 0.39; IR ν (cm^{-1}) 3422 (O–H), 2805, 1727 (C=O), 1373, 1181 (C–O); NMR δ_{H} (400 MHz; CDCl_3) 7.38–7.22 (5H, m, Ph), 4.53–4.49 (1H, m, H-4), 4.20 (2H, q, J 7.0 Hz, CH_2CH_3), 3.72 (1H, d, J 13.0 Hz, PhCHH-), 3.67 (1H, d, J 13.0 Hz, PhCHH-), 3.19–3.10 (1H, m, H-3), 3.09–3.01 (1H, m, H-2a), 2.89 (1H, dd, J 10.0, 5.0 Hz, H-5a), 2.75 (1H, t, J 9.0 Hz, H-2b), 2.64 (1H, dd, J 10.0, 3.0 Hz, H-5b), 1.28 (3H, t, J 7.0 Hz, CH_3CH_2); δ_{C} (101 MHz, CDCl_3) 172.1 (CO), 138.5 (Ph), 128.7 (Ph), 128.3 (Ph), 127.1 (Ph), 71.7 (C-4), 61.7 (C-5), 60.9 (CH_2CH_3), 59.8 (PhCH₂), 53.5 (C-2), 48.8 (C-3), 14.2 (CH_3CH_2); GC–MS t_{R} = 20.8 min. m/z (EI) 249 (M^+ , 4%), 204 (10%), 158 (50%), 133 (12%), 132 (17%), 91 (PhCH₂⁺, 100%), 65 (10%); HRMS (ESI) m/z calcd for $\text{C}_{14}\text{H}_{20}\text{NO}_3$ [$\text{M} + \text{H}$]⁺ 250.1438, found 250.1427.

6.11. Ethyl *rel*-(3R,4S)-1-benzyl-4-hydroxypyrrolidine-3-carboxylate ((±)-13)

Further elution, of the column described above, with Pet. Ether/EtOAc [1:1] 1% Et_3N gave the *trans* product (±)-**13** as a yellow oil (0.91 g, 37%); R_f (Pet. Ether/EtOAc [1:1], 1% Et_3N) 0.10; IR ν (cm^{-1}) 3385 (O–H), 2979, 2932, 2799, 1727 (C=O), 1454, 1372, 1255, 1178 (C–O), 1027; NMR δ_{H} (400 MHz; CDCl_3) 7.33–7.22 (5H, m, Ph), 4.51 (1H, dt, J 5.5, 3.0 Hz, H-4), 4.16 (2H, q, J 7.0 Hz, CH_2CH_3), 3.63 (2H, s, PhCH₂-), 3.12 (1H, t, J 9.5 Hz, H-2a), 2.95 (1H, dt, J 8.0, 3.5 Hz, H-3), 2.76 (1H, dd, J 10.0, 3.0 Hz, H-5a), 2.64 (1H, dd, J 10.0, 5.5 Hz, H-5b), 2.54 (1H, dd, J 9.5, 7.5 Hz, H-2b), 2.32 (1H, bs, OH, exchanged with D₂O), 1.26 (3H, t, J 7.0 Hz, CH_3CH_2); δ_{C} (101 MHz, CDCl_3) 173.2 (CO), 138.3 (Ph), 128.7 (Ph), 128.3 (Ph), 127.1 (Ph), 74.3 (C-4), 61.8 (C-5), 60.9 (CH_2CH_3), 59.6 (benzyl CH₂), 55.2 (C-2), 53.1 (C-3), 14.2 (CH_3CH_2); GC–MS t_{R} = 20.1 min. m/z (EI) 249 (M^+ , 12%), 220 (10%), 204 (20%), 158 (79%), 133 (20%), 132 (26%), 91 (PhCH₂⁺, 100%), 65 (14%); NMR data agrees with that reported in the literature.⁴²

6.12. Epimerisation study 12 → 13 (Table 1, entry 6)

A 0.1 M solution of EtONa was prepared by the addition of sodium (9 mg, 0.4 mmol) to anhydrous ethanol (4 mL) under nitrogen. After complete consumption of the sodium, part of the resulting solution (0.8 mL, 80 μmol) was transferred to a flask containing *cis*-pyrrolidine **12** (20 mg, 80 μmol) and the resulting solution was stirred at RT for 18 h. DCM (2 mL) was added to produce a precipitate which was removed by filtration through Celite®. The filtrate was evaporated to dryness and analysed by ¹H NMR.

6.13. Ethyl (3R,4S)-4-(acetyloxy)-1-benzylpyrrolidine-3-carboxylate ((-)-14)

Vinyl acetate (2.18 mL) and lipase from *Candida antarctica* (1.37 g, Sigma Aldrich, batch SLBG4222V) were added to a solution of (±)-**8** (1.96 g, 7.88 mmol) in *tert*-butyl methyl ether (62 mL). The mixture was stirred at $40\text{ }^{\circ}\text{C}$ for 2.5 h and filtered through Celite®. The solids were washed with EtOAc and the combined filtrates were washed using saturated NaHCO_3 solution, dried over anhydrous MgSO_4 , filtered, concentrated and dried *in vacuo* to afford a yellow oil. Flash column silica chromatography of the resulting mixture (Pet. Ether/EtOAc [3:2]) gave first acetate (–)-**14** as a yellow oil (0.85 g, 75%); R_f (Pet. Ether/EtOAc [3:2]) 0.73; IR ν (cm^{-1}) 2979, 2799, 1732 (C=O), 1454, 1370, 1234 (C–O), 1194, 1174 (C–O), 1029; NMR δ_{H} (400 MHz; CDCl_3) 7.33–7.25 (5H, m, Ph), 5.40 (1H, dt, J 6.5, 3.0 Hz, H-4), 4.17 (2H, q, J 7.0 Hz, CH_2CH_3), 3.65 (1H, d, J 13.0 Hz, PhCHH-), 3.59 (1H, d, J 13.0 Hz, PhCHH-), 3.16 (1H, t, J 8.5 Hz, H-2a), 3.06 (1H, td, J 8.0, 3.5 Hz, H-3), 2.82 (1H, dd, J 11.0, 2.5 Hz, H-5a), 2.76 (1H, dd, J 11.0, 6.0 Hz, H-5b), 2.49 (1H, dd, J 9.0, 8.5 Hz, H-2b), 2.05 (3H, s, COCH_3), 1.26 (3H, t, J 7.0 Hz, CH_3CH_2); δ_{C} (126 MHz, CDCl_3) 172.4 (CO), 170.7 (CO), 138.0 (Ph), 128.8 (Ph), 128.3 (Ph), 127.2 (Ph), 76.1 (C-4), 61.1 (CH_2CH_3), 59.7 (C-5), 59.6 (PhCH₂-), 56.1 (C-2), 50.2 (C-3), 21.1 (COCH_3), 14.2 (CH_2CH_3); GC–MS t_{R} = 21.7 min. m/z (EI) 291 (M^+ , 0.5%), 231 (18%), 159 (13%), 158 (98%), 91 (100%); $[\alpha]_{\text{D}}^{20}$ = -40.7 (c 1.40 CHCl_3) (lit.⁴², $[\alpha]_{\text{D}}^{20}$ = -41.8 (c 0.895, CHCl_3)); HRMS (ESI) m/z calcd for $\text{C}_{16}\text{H}_{22}\text{NO}_4$ [$\text{M} + \text{H}$]⁺ 292.1543, found 292.1526. NMR and $[\alpha]_{\text{D}}^{20}$ agrees with that published in the literature.⁴²

6.14. Ethyl (3S,4R)-1-benzyl-4-hydroxypyrrolidine-3-carboxylate ((+)-13)

Further elution, of the column described above, with Pet. Ether/EtOAc [1:4] gave hydroxypyrrolidine (+)-**13** as a colourless gum, which crystallised at $-20\text{ }^{\circ}\text{C}$ (0.82 g, 83%); m.p. $48\text{--}50\text{ }^{\circ}\text{C}$ (lit.⁴² $51\text{--}52\text{ }^{\circ}\text{C}$); R_f (Pet. Ether/EtOAc [3:2]) 0.20; IR ν (cm^{-1}) 3414 (O–H), 2974, 2799, 1727 (C=O), 1454, 1372, 1242, 1178 (C–O), 1029; NMR

δ_{H} (400 MHz; CDCl_3) 7.33–7.27 (5H, m, Ph), 4.51 (1H, dt, J 5.5, 3.0 Hz, H-4), 4.16 (2H, q, J 7.0 Hz, CH_2CH_2), 3.68 (1H, d, J 13.0 Hz, PhCHH-), 3.64 (1H, d, J 13.0 Hz, PhCHH-), 3.16 (1H, t, J 9.0 Hz, H-2a), 2.97 (1H, td, J 8.0, 3.0 Hz, H-3), 2.80 (1H, dd, J 10.0, 2.5 Hz, H-5a), 2.66 (1H, dd, J 10.0, 5.5 Hz, H-5b), 2.57 (1H, dd, J 9.5, 7.5 Hz, H-2b), 2.07 (1H, bs, OH, exchanged with D_2O), 1.26 (3H, t, J 7.0 Hz, CH_3CH_2); δ_{C} (126 MHz, CDCl_3) 173.2 (C=O), 138.3 (Ph), 128.7 (Ph), 128.3 (Ph), 127.1 (Ph), 74.3 (C-4), 61.8 (PhCH $_2$ -), 60.9 (CH_2CH_3), 59.6 (C-5), 55.2 (C-3), 53.1 (C-2), 14.2 (CH_2CH_3); GC-MS $t_{\text{R}} = 20.8$ min. m/z (EI) 249 (M^+ , 2%), 229 (11%), 184 (12%), 158 ($[\text{M}-\text{PhCH}_2]^+$, 25%), 91 (PhCH $_2^+$, 100%), 65 (11%); $[\alpha]_{\text{D}}^{20} + 19.5$ (c 0.91 CHCl_3) (lit.⁴² $[\alpha]_{\text{D}}^{20} + 16.9$ (c 0.71, CHCl_3)); NMR and $[\alpha]_{\text{D}}^{20}$ data agrees with that reported in the literature.⁴²

6.15. (3*R*,4*R*)-1-Benzyl-4-(hydroxymethyl)pyrrolidin-3-ol ((+)-15)

Hydroxypyrrolidine (+)-13 (0.48 g, 1.91 mmol) was dissolved in dry THF (15.6 mL) and cooled to 0 °C. LiAlH_4 (0.29 g, 7.62 mmol) was added slowly and the mixture was warmed to RT and stirred until LCMS showed reaction completion (~2 h). The mixture was diluted with ether and excess hydride was quenched at 0 °C by successive addition of water (0.3 mL), aqueous NaOH solution (15%, 0.3 mL) and water (0.9 mL). Then, the mixture was warmed to RT, stirred for 15 min, dried over anhydrous MgSO_4 , filtered, concentrated and dried *in vacuo*. Flash column silica chromatography (DCM/MeOH [9:1]) gave diol (+)-15 as a colourless gum (0.28 g, 71%); R_{f} (DCM/MeOH [9:1]) 0.14; δ_{H} (400 MHz; CD_3OD) 7.36–7.27 (5H, m, Ph), 4.00 (1H, dt, J 6.0, 4.0 Hz, H-3), 3.68 (1H, d, J 12.5 Hz, PhCHH-), 3.65 (1H, dd, J 10.5, 5.5 Hz, -CHHOH), 3.58 (1H, d, J 12.5 Hz, PhCHH-), 3.51 (1H, dd, J 10.5, 7.5 Hz, -CHHOH), 2.92 (1H, dd, J 9.5, 8.0 Hz, H-5a), 2.75 (1H, dd, J 10.0, 6.0 Hz, H-2a), 2.59 (1H, dd, J 10.0, 4.0 Hz, H-2b), 2.37 (1H, dd, J 9.5, 6.5 Hz, H-5b), 2.24–2.16 (1H, m, H-4); δ_{C} (101 MHz, CDCl_3) 137.8 (Ph), 128.9 (Ph), 128.4 (Ph), 127.3 (Ph), 74.2 (C-3), 64.6 (CH_2O), 62.3 (C-2), 60.1 (PhCH $_2$ -), 55.9 (C-5), 50.0 (C-4); GC-MS $t_{\text{R}} = 20.1$ min. m/z (EI) 207 (M^+ , 3%), 133 (8%), 132 (11%); 91 (PhCH $_2^+$, 100%), 77 (Ph $^+$, 5%), 65 (19%); $[\alpha]_{\text{D}}^{20} + 31.1$ (c 1.01 MeOH) (lit.⁴² $[\alpha]_{\text{D}}^{20} + 33.0$ (c 0.75 MeOH)); HRMS (ESI) m/z calcd for $\text{C}_{12}\text{H}_{18}\text{NO}_2$ $[\text{M}+\text{H}]^+$ 208.1332, found 208.1314; NMR data agrees with that reported in the literature.⁴²

6.16. *tert*-Butyl (3*R*,4*R*)-3-[(*tert*-butoxycarbonyl)oxy]-4-[[(*tert*-butoxycarbonyl)oxymethyl]pyrrolidine-1-carboxylate (16)

Pd/C (10% w/w, 0.057 g, 10%) was added to a stirred solution of diol (+)-15 (0.28 g, 1.37 mmol) and di-*tert*-butyl dicarbonate (0.66 mL, 2.84 mmol) in MeOH (5.7 mL).⁴² The atmosphere was replaced with H_2 (balloon) and the reaction mixture was stirred for 24 h. The mixture was filtered through Celite®, the solvent was evaporated and the residue was subjected to flash column chromatography (EtOAc/MeOH [2:1]) to afford firstly tris-Boc compound 16 as a colourless gum (0.25 g, 44%); R_{f} (Pet. ether/EtOAc [2:1]) 0.72; IR ν (cm^{-1}) 3321 (O-H), 2945, 2764, 1616 (C=O), 1454, 1400, 1065, 1047 (C-O); NMR (400 MHz; CDCl_3) 4.88 (1H, dt, J 5.5, 3.0 Hz, H-3), 3.93 (2H, dd, J 7.0, 2.5 Hz, CH_2O), 3.61 (1H, dd, J 12.5, 5.5 Hz, H-2a), 3.52 (1H, dd, J 11.0, 7.5 Hz, H-5a), 3.42–3.31 (1H, m, H-2b), 3.25–3.16 (1H, m, H-5b), 2.60–2.57 (1H, m, H-4), 1.39 (18H, s, 2 \times $\text{C}(\text{CH}_3)_3$), 1.36 (9H, s, $\text{C}(\text{CH}_3)_3$); δ_{C} (101 MHz, CDCl_3) 153.9 (CO), 153.0 (CO), 152.4 (CO), 82.5 ($\text{C}(\text{CH}_3)_3$), 82.2 ($\text{C}(\text{CH}_3)_3$), 79.4 ($\text{C}(\text{CH}_3)_3$), 75.9 (C-3), (65.4, 65.3) (CH_2O), (50.3, 50.1) (C-2), (46.4, 45.9) (C-5), (43.1, 42.2) (C-4), 28.2 ($\text{C}(\text{CH}_3)_3$), 27.5 ($\text{C}(\text{CH}_3)_3$), 27.5 ($\text{C}(\text{CH}_3)_3$); HRMS (ESI) *Molecular ion not detected*.

6.17. *tert*-Butyl (3*R*,4*R*)-3-hydroxy-4-(hydroxymethyl)pyrrolidine-1-carboxylate ((+)-17)

Pd/C (0.010 g, 10%) was added to a stirred solution of the diol

(+)-15 (0.050 g, 0.24 mmol) and di-*tert*-butyl dicarbonate (0.06 mL, 0.24 mmol) in MeOH (1 mL).⁴² The atmosphere was replaced with H_2 (balloon) and the reaction mixture was stirred for 24 h. The mixture was filtered through Celite®, the solvent was evaporated and the residue was subjected to flash column chromatography (AcOEt/MeOH [35:1]) to afford *N*-Boc pyrrolidine (+)-17 as a colourless gum (0.028 g, 54%); R_{f} (Pet. ether/EtOAc [2:1]) 0.24; NMR δ_{H} (500 MHz; CDCl_3) 4.29–4.22 (1H, m, H-3), 3.72–3.57 (4H, m, CH_2O , H-2, H-5), 3.29–3.21 (1H, m, H-2), 3.12–3.09 (1H, m, H-5), 3.10 (0.5H, bs, OH, exchanged with D_2O), 2.94 (0.5H, bs, OH, exchanged with D_2O), 2.69 (0.5H, bs, OH, exchanged with D_2O), 2.51 (0.5H, bs, OH, exchanged with D_2O), 2.35–2.28 (1H, m, H-4), 1.45 (9H, s, $\text{C}(\text{CH}_3)_3$); δ_{C} (126 MHz, CDCl_3) 154.7 (CO), 79.7 ($\text{C}(\text{CH}_3)_3$), (73.2, 72.3) (C-3), 63.0 (CH_2O), (52.7, 52.3) (C-2), (48.2, 47.6) (C-4), (46.6, 46.0) (C-5), 28.5 ($\text{C}(\text{CH}_3)_3$); GC-MS $t_{\text{R}} = 19.2$ min. m/z (EI) 217 (M^+ , 1%), 144 (19%), 112 (11%), 68 (15%), 57 (100%), 56 (46%), 55 (21%); $[\alpha]_{\text{D}}^{20} + 23.2$ (c 1.00 MeOH) (lit.³⁸ $[\alpha]_{\text{D}}^{20} + 16$ (c 0.8 MeOH)); NMR data agrees with that reported in the literature.⁶⁷

6.18. (3*R*,4*R*)-4-(Hydroxymethyl)pyrrolidin-3-ol hydrochloride ((+)-18-HCl)

6.18.1. Method 1

N-Boc pyrrolidine (+)-17 (0.026 g, 0.120 mmol) was dissolved in MeOH (2 mL) and aqueous HCl (37%, 1 mL) was added at RT.⁴² The mixture was stirred for 1 h and the solvent was evaporated to give the title compound as a yellow oil (0.018 g, > 99%); NMR δ_{H} (400 MHz; D_2O) 4.44–4.35 (1H, m, H-3), 3.64–3.55 (3H, m, CH_2O , H-2), 3.42 (1H, dd, J 12.5, 4.5 Hz, H-5), 3.25 (1H, d, J 12.5 Hz, H-5), 3.15 (1H, dd, J 12.0, 5.5 Hz, H-2), 2.52–2.38 (1H, m, H-4); δ_{C} (101 MHz, D_2O) 71.4 (C-3), 60.4 (CH_2O), 51.6 (C-5), 47.4 (C-4), 46.1 (C-2); $[\alpha]_{\text{D}}^{20} + 16.0$ (c 1.00 MeOH) (lit.⁴⁰ $[\alpha]_{\text{D}}^{20} + 19.0$ (c 1.0, MeOH)); HRMS (ESI) m/z calcd for $\text{C}_5\text{H}_{12}\text{NO}_2$ $[\text{M}+\text{H}]^+$ 118.0863, found 118.0861; all data agrees with that reported in the literature.^{40,53}

6.18.2. Method 2

Pd/C (10% w/w, 0.091 g) was added to a stirred solution of diol (+)-15 (0.45 g, 2.18 mmol) and di-*tert*-butyl dicarbonate (0.52 mL, 2.27 mmol) in MeOH (9.1 mL).⁴² The atmosphere was replaced with H_2 (balloon) and the reaction mixture was stirred for 24 h. The mixture was filtered through Celite® and the solvent was evaporated to give the crude product (0.44 g) which was dissolved in MeOH (17.3 mL) and aqueous HCl (37%, 8.7 mL) was added at RT. The mixture was stirred for 30 min and the solvent was evaporated to give the title compound in pure form as a yellow oil (0.24 g, 78%); NMR data was identical to that from Method 1, above.

6.19. General procedure for reductive amination to give test inhibitors 6a–6e

To a solution of pyrrolidine hydrochloride (+)-18.HCl (50 mg, 0.33 mmol) in anhydrous MeOH (2.2 mL) was added the appropriate aryl aldehyde (1.07 equiv., 0.35 mmol) and the mixture stirred at RT until complete dissolution. Then, NaBH_3CN was added portionwise and the mixture was left stirring under N_2 for 18 h. General work-up involved filtration of the mixture through Celite® and solvent evaporation.

6.20. (3*R*,4*R*)-4-(Hydroxymethyl)-1-[(1*H*-imidazol-2-yl)methyl]pyrrolidin-3-ol (+)-6a

The general procedure for reductive amination was followed. The resulting crude product was adsorbed onto silica and flash column silica chromatography was performed (DCM/MeOH [19:1] to [7:3]) to give the title compound as a yellow oil (36 mg, 56%); R_{f} (DCM/MeOH [5:1]) 0.15; NMR δ_{H} (400 MHz, MeOD) 7.02 (2H, s, Ar-H), 4.08–4.01 (1H, m, H-3), 3.79 (1H, d, J 14.0 Hz, ArCHH-), 3.74 (1H, d, J 14.0 Hz, ArCHH-),

3.60 (1H, dd, *J* 11.0, 6.0 Hz, CHHO), 3.52 (1H, dd, *J* 11.0, 7.0 Hz, CHHO), 3.01 (1H, t, *J* 9.0 Hz, H-5a), 2.77 (1H, dd, *J* 10.0, 6.0 Hz, H-2a), 2.68 (1H, dd, *J* 10.0, 3.5 Hz, H-2b), 2.38 (1H, dd, *J* 9.5, 7.0 Hz, H-5b), 2.26–2.17 (1H, m, H-4); δ_C 101 MHz, MeOD) 146.3 (Ar), 122.8 (Ar), 74.3 (C-3), 64.0 (CH₂O), 62.9 (C-2), 57.1 (C-5), 52.8 (ArCH₂-), 51.4 (C-4); [α_D^{20} + 16.0 (c 4.85 MeOH); HRMS (ESI) *m/z* calcd for C₉H₁₆N₃O₂ [M+H]⁺ 198.1237, found 198.1235.

6.21. (3*R*,4*R*)-4-(Hydroxymethyl)-1-[(1*H*-imidazol-4-yl)methyl]pyrrolidin-3-ol ((+)-6b)

The general procedure for reductive amination was followed. As soon as NaBH₃CN was added, the mixture, initially a transparent solution, turned cloudy. After stirring at RT for 22 h, LCMS revealed a high concentration of unreacted starting material. For that reason, 1 extra equiv. of 1*H*-Imidazole-4-carbaldehyde was added (31 mg, 0.33 mmol) and the mixture was stirred for 1 h. It was then filtered through Celite® and loaded onto a 2 g strong cation exchange column. Elution with MeOH followed by NH₃ solution (1 M in MeOH) gave the title compound as a yellow oil (11 mg, 17%); R_f [DCM/MeOH (5:1)] 0.28; NMR δ_H (400 MHz, MeOD) 7.61 (1H, d, *J* 1.0 Hz, Ar-*H*), 6.97 (1H, s, Ar-*H*) 3.98 (1H, dt, *J* 6.0, 4.0 Hz, H-3), 3.64 (1H, d, *J* 13.5 Hz, ArCHH-), 3.61 (1H, dd, *J* 11.0, 6.0 Hz, CHHO), 3.57 (1H, d, *J* 13.5 Hz, ArCHH-), 3.49 (1H, dd, *J* 10.5, 7.5 Hz, CHHO), 2.93 (1H, dd, *J* 9.5, 8.5 Hz, H-5a), 2.74 (1H, dd, *J* 10.0, 6.0 Hz, H-2a), 2.60 (1H, dd, *J* 10.0, 4.0 Hz, H-2b), 2.35 (1H, dd, *J* 9.5, 6.5 Hz, H-5b), 2.20–2.12 (1H, m, H-4); δ_C (101 MHz, MeOD) 136.3 (Ar), 134.9 (Ar), 120.2 (Ar), 74.2 (C-3), 64.3 (CH₂O), 62.8 (C-2), 57.0 (C-5), 52.3 (ArCH₂-), 51.3 (C-4); [α_D^{20} + 150.1 (c 1.00 MeOH); HRMS (ESI) *m/z* calcd for C₉H₁₆N₃O₂ [M+H]⁺ 198.1237, found 198.1242.

6.22. (3*R*,4*R*)-4-(Hydroxymethyl)-1-[(pyridin-2-yl)methyl]pyrrolidin-3-ol ((+)-6c)

The general procedure for reductive amination was followed. The crude product was purified by flash column silica chromatography (DCM/MeOH [9:1]) to give the title compound as a yellow oil (39 mg, 61%); R_f 0.2 (DCM/MeOH [9:1]); NMR δ_H (400 MHz, D₂O) 8.44–8.42 (2H, m, Ar-*H*), 7.80 (1H, ddd, *J* 8.0, 2.0, 1.5 Hz, Ar-*H*), 7.42 (1H, ddd, *J* 8.0, 5.0, 0.5 Hz, Ar-*H*) 4.05 (1H, dt, *J* 6.0, 4.5 Hz, H-3), 3.71 (1H, d, *J* 13.0 Hz, ArCHH-), 3.63 (1H, dd, *J* 11.0, 6.5 Hz, CHHO), 3.60 (1H, d, *J* 13.0 Hz, ArCHH-), 3.52 (1H, dd, *J* 11.0, 7.5 Hz, CHHO), 2.93 (1H, dd, *J* 10.0, 8.0 Hz, H-5a), 2.78 (1H, dd, *J* 10.5, 6.5 Hz, H-2a), 2.60 (1H, dd, *J* 10.5, 4.0 Hz, H-2b), 2.31 (1H, dd, *J* 10.0, 7.0 Hz, H-5b), 2.23–2.15 (1H, m, H-4); δ_C (101 MHz, D₂O) 149.3 (Ar), 147.8 (Ar), 138.6 (Ar), 133.1 (Ar), 124.1 (Ar), 72.4 (C-3), 62.4 (CH₂O), 60.5 (C-2), 56.6 (ArCH₂-), 55.2 (C-5), 48.5 (C-4); [α_D^{20} + 13.6 (c 1.00 MeOH); HRMS (ESI) *m/z* calcd for C₁₁H₁₇N₂O₂ [M+H]⁺ 209.1285, found 209.1291.

6.23. (3*R*,4*R*)-4-(Hydroxymethyl)-1-[(pyridin-3-yl)methyl]pyrrolidin-3-ol ((+)-6d)

The general procedure for reductive amination was followed. The crude product was purified by flash column silica chromatography (DCM/MeOH [9:1]) to yield a yellow oil which was characterised as a mixture of title compound and borohydride salts. Addition of MeOH (1 mL) left an insoluble component which was removed by filtration through Celite®. Evaporation of the filtrate gave the title compound (28 mg, 44%); R_f 0.15 (DCM/MeOH [9:1]); NMR δ_H (400 MHz, MeOD) 8.54 (1H, d, *J* 4.5 Hz, Ar-*H*), 7.84 (1H, td, *J* 7.5, 1.5 Hz, Ar-*H*), 7.52 (1H, d, *J* 8.0 Hz, Ar-*H*) 7.36 (1H, dd, *J* 7.5, 5.0 Hz, Ar-*H*), 4.15 (1H, dt, *J* 6.0, 3.5 Hz, H-3), 4.10 (1H, d, *J* 14.0 Hz, ArCHH-), 4.02 (1H, d, *J* 14.0 Hz, ArCHH-), 3.64 (1H, dd, *J* 11.0, 5.5 Hz, CHHO), 3.57 (1H, dd, *J* 10.5, 6.5 Hz, CHHO), 3.26 (1H, dd, *J* 10.0, 8.5 Hz, H-5a), 3.06 (1H, dd, *J* 10.5, 6.0 Hz, H-2a), 2.91 (1H, dd, *J* 10.5, 3.0 Hz, H-2b), 2.73 (1H, dd, *J* 10.5, 6.5 Hz, H-5b), 2.36–2.26 (1H, m, H-4); δ_C (101 MHz, MeOD)

157.0 (Ar), 150.2 (Ar), 139.0 (Ar), 125.0 (Ar), 124.5 (Ar), 73.9 (C-3), 63.4 (CH₂O), 63.1 (C-2), 61.7 (ArCH₂-), 57.4 (C-5), 50.9 (C-4); [α_D^{20} + 154.2 (c 1.00 MeOH); HRMS (ESI) *m/z* calcd for C₁₁H₁₇N₂O₂ [M+H]⁺ 209.1285, found 209.1292.

6.24. (3*R*,4*R*)-4-(hydroxymethyl)-1-[(pyridin-4-yl)methyl]pyrrolidin-3-ol ((+)-6e)

The general procedure for reductive amination was followed. Upon addition of NaBH₃CN, the mixture, initially an orange solution, turned yellow. After 18 h the bright yellow suspension was filtered through Celite® and the solvent was removed. In order to remove the boron salts present in the crude product, the residue was taken up in water (5 mL) and the pH was adjusted to 10 using aqueous NaOH solution (1 M). This was extracted with DCM/MeOH (9:1, 3 × 10 mL) and the combined organic layers were washed with brine (30 mL). Flash column silica chromatography (DCM/MeOH [9:1]) gave the title compound and 4-pyridinemethanol. Further chromatography (DCM/MeOH [3:1]) gave the title compound as a yellow oil (10 mg, 16%); R_f 0.31 (DCM/MeOH [3:1]); NMR δ_H (400 MHz, MeOD) 8.47 (2H, d, *J* 6.0 Hz, Ar-*H*), 7.46 (2H, d, *J* 6.0 Hz, Ar-*H*), 4.04 (1H, dt, *J* 6.0, 3.5 Hz, H-3), 3.76 (1H, d, *J* 14.0 Hz, ArCHH-), 3.66 (1H, d, *J* 14.0 Hz, ArCHH-), 3.63 (1H, dd, *J* 11.0, 6.0 Hz, CHHO), 3.53 (1H, dd, *J* 10.5, 7.5 Hz, CHHO), 2.96 (1H, dd, *J* 9.0, 8.5 Hz, H-5a), 2.77 (1H, dd, *J* 10.0, 6.0 Hz, H-2a), 2.63 (1H, dd, *J* 10.0, 3.5 Hz, H-2b), 2.39 (1H, dd, *J* 9.5, 6.5 Hz, H-5b), 2.26–2.18 (1H, m, H-4); δ_C (101 MHz, MeOD) 150.3 (Ar), 150.1 (Ar), 125.6 (Ar), 74.1 (C-3), 64.0 (CH₂O), 63.1 (C-2), 59.9 (ArCH₂-), 57.3 (C-5), 51.3 (C-4); [α_D^{20} + 231.7 (c 1.00 MeOH); HRMS (ESI) *m/z* calcd for C₁₁H₁₇N₂O₂ [M+H]⁺ 209.1285, found 209.1297.

6.25. AAG inhibitor biochemical assay

6.25.1. Materials

Nunc® Immobiliser™ Amino 96-well plates were purchased from ThermoFisher Scientific (Hemel Hemstead, UK). T4 DNA ligase was purchased from Promega (Southampton, UK). It was supplied in a storage buffer containing 10 mM Tris-HCl (pH 7.4), 50 mM KCl, 1 mM dithiothreitol (DTT), 0.1 mM ethylenediaminetetraacetic acid (EDTA) and 50% glycerol. Oligonucleotides HX02 and Loop01 were purchased from Integrated DNA Technologies (Leuven, Belgium). They were supplied lyophilised and were suspended in ultrapure (Milli-Q®) water to 1 mM, and subsequently diluted to 10 μM solutions in the corresponding buffer. Their sequences (5' to 3') are given below:*

HX02: (P)CACGAHCAACTCAGCAACTCCtt(NH₂)

Loop01: (flc)ttGGAGTTGCTGAGTTGATTCTGTGAGCACCAACCGGT GCT.

AAG enzyme (10,000 U/mL)§ was purchased from New England Biolabs (Hitchin, UK). It was supplied in a storage buffer containing 100 mM KCl, 10 mM Tris-HCl (pH 7.4), 0.1 mM EDTA, 1 mM DTT, 0.5% Tween® 20, 0.5% NP-40 and 50% glycerol.

Goat antibody to fluorescein (goat anti-fluorescein) horseradish peroxidase (1 mg/mL) was purchased from Abcam (Cambridge, UK). It was supplied in a storage buffer containing 0.42% potassium phosphate (pH 7.2), 0.87% sodium chloride, 1% BSA and 0.1% Gentamicin as a preservative. It was diluted 10-fold into PBST containing 1% w/v BSA and stored as single use aliquots at –20 °C. 3,3',5,5'-Tetramethylbenzidine (TMB) peroxidase substrate solution and peroxidase substrate buffer were purchased from Insight Biotechnology Ltd (Wembley, UK).

Bicarbonate buffer was prepared by dissolving 0.18 g of NaHCO₃ and 0.04 g of Na₂CO₃ in 50 mL milliQ water (pH = 9.6). Phosphate

* DNA oligomer sequences: lower case letters indicate nucleotides linked via phosphorothiate bonds; X = hypoxanthine; (P) = phosphate; (NH₂) = amino modifier group (CH₂CH(OH)CH₂O(CH₂)₃NH₂); (flc) = fluorescein.

buffered saline 0.1% v/v Tween® 20 (PBST) was prepared by dilution of 1 mL Tween® 20 (Sigma-Aldrich) in 1 L of ultrapure (Milli-Q®) water which contained 10 PBS tablets (Sigma-Aldrich). AAG glycosylase buffer was prepared by mixing 4 mL Tris 1 M (pH 7.8) (Sigma-Aldrich), 20 mL KCl 1 M, 4 mL EDTA 0.25 M (pH 8) (Sigma-Aldrich), 400 µL egtazic acid (EGTA) 500 mM (Sigma-Aldrich) and 69.6 µL of β-mercaptoethanol (Sigma-Aldrich) in 171.5 mL ultrapure (Milli-Q®) water. Hybridisation buffer was prepared by mixing 30 mL 20xSSC (Sigma-Aldrich), 0.1 mL Tween® 20, 1 mL EDTA 0.5 M and 68.9 mL ultrapure (Milli-Q®) water. T4 ligase buffer was prepared by diluting 6 mL Tris 1 M (pH 7.8), 6 mL NaCl 1 M, 2 mL MgCl₂ 1 M in 186 mL ultrapure (Milli-Q®) water. DNA ligase buffer was prepared by mixing 47.424 mL T4 ligase buffer, 480 µL DTT (1 M) and 96 µL ATP (Sigma-Aldrich). Alkaline denaturation buffer was prepared by diluting 10 mL NaOH 5 M and 2.5 20xSSC in 487.5 mL ultrapure (Milli-Q®) water.

6.25.2. Procedure

Step 1: Binding of HX02 substrate oligonucleotide to well surface A 0.5 nM solution of oligonucleotide HX02 was prepared by diluting 10 µM HX02 into bicarbonate buffer. It was added to the Nunc® Immobiliser™ Amino plate (100 µL 0.5 nM, 0.05 pmol HX02 per well), which was incubated overnight at 4 °C. Then, the liquid was decanted from the wells and the plate was washed with PBST (3 × 150 µL/well) and dried.

Step 2: In situ hybridisation of HX02 and Loop01

A 0.5 nM solution of oligonucleotide Loop01 was prepared by diluting 10 µM Loop01 into hybridisation buffer. It was added to the plate (100 µL 0.5 nM, 0.05 pmol Loop01 per well), which was heated to 95 °C for 10 min. Then, it was cooled to 80 °C and kept at 80 °C for 10 min. After this time, it was cooled to 70 °C, 60 °C, 50 °C, 40 °C and 30 °C each for 10 min to promote annealing of the DNA strands. It was allowed to cool to RT, the liquid was decanted, the plate was washed with PBST (3 × 150 µL/well) and dried by vigorous tapping onto paper towel.

Step 3: Ligation reaction

A 0.04 U/100 µL solution of T4 DNA ligase was prepared by diluting 3 U/µL T4 DNA ligase into ligase buffer. It was added to the plate (100 µL/well), which was incubated at 37 °C for 2 h. The liquid was decanted and the plate was washed with PBST (3 × 150 µL/well). The final wash was left in the wells and the plates were frozen overnight. Then, they were warmed to RT, emptied and dried by vigorous tapping onto paper towel.

Step 4: AAG standard preparations with BSA

A 100 µg/mL BSA in glycosylase buffer was prepared. This solution was used to prepare increasing concentrations of the different inhibitors which were tested against AAG.

A 0.8 U/100 µL stock solution of AAG was prepared by diluting 10 U/µL purchased AAG into AAG glycosylase buffer/BSA. Increasing concentrations of AAG (0 U/well to 0.4 U/well) were prepared by diluting the stock solution into AAG glycosylase buffer/BSA. 0.05 U/100 µL AAG was the concentration selected at which to test the different inhibitors. Each mixture of enzyme and inhibitor was allowed at least 5 min of pre-incubation time.

Step 5: Incubation and work-up

The different AAG (+/- inhibitor) dilutions were added to the plate (100 µL/well), each with three replicates, which was incubated at 37 °C for 2 h. Then, the liquid was decanted, the plate was washed with PBST (3 × 150 µL) and dried. Alkaline denaturation buffer was added (200 µL/well) and the plate was incubated at 95 °C for 15 min. Then, it was allowed to cool to RT, the liquid was decanted, the plate was washed with PBST (3 × 200 µL/well) and dried.

Step 6: Colorimetric detection

A solution of BSA in PBST (10 mL, 0.01 g/mL) was prepared. Then, 10 µL of 1:10 diluted goat antibody to fluorescein (goat anti-fluorescein) horseradish peroxidase was added. This solution was added to the plate (100 µL/well), which was incubated at RT for 1 h. Then, the liquid was decanted, the plate was washed with PBST (3 × 200 µL/

well) and dried. A 1:1 mixture of TMB peroxidase substrate solution and peroxidase substrate buffer was prepared. It was added to the plate (100 µL/well). Once sufficient pale blue colour had developed (12 min), phosphoric acid 1 M (100 µL/well) was added, and a colour change to yellow was observed. The absorbance was read at 450 nm.

Step 7: Data processing

GraphPad Prism 7.04 was used to process the data. A standard curve of absorbance vs. [AAG] was plotted and absorbances acquired from wells containing inhibitor were interpolated into this to obtain an apparent [AAG]. The values of apparent [AAG] were used to calculate the % inhibition given that a real [AAG] of 0.05 U/100 µL was used. IC₅₀ curves of the proposed inhibitors were fitted using equation: "[Inhibitor] vs. response" which also generated IC₅₀ values from the mid-point between the top and bottom of the curve (not the y = 50% mark).

Declaration of Competing Interest

The authors declare that there are no conflicts of interest.

Acknowledgements

D. Whelligan and R. Elliott thank the Royal Society for a research grant for part of this work. The EPSRC is gratefully acknowledged for the "MILES" grant (EP/I000992/1), part of which helped fund development of the biochemical assay and a summer research project for S. Chu. E. Mas thanks the University of Surrey, U.K. for funding of a PhD scholarship. B. Al Yahyaie thanks the Sultanate of Oman for funding of a PhD scholarship. M. Imperato and A. Lopez thank the Erasmus + scheme for funding of summer research projects.

Appendix A. Supplementary material

Supplementary data to this article can be found online at <https://doi.org/10.1016/j.bmc.2020.115507>.

References

- Fu D, Calvo JA, Samson LD. Balancing repair and tolerance of DNA damage caused by alkylating agents. *Nat Rev Cancer*. 2012;12:104–120. <https://doi.org/10.1038/nrc3185>.
- Meira LB, Moroski-Erkul CA, Green SL, et al. Aag-initiated base excision repair drives alkylation-induced retinal degeneration in mice. *Proc Natl Acad Sci*. 2009;106:888–893. <https://doi.org/10.1073/pnas.0807030106>.
- Calvo JA, Moroski-Erkul CA, Lake A, et al. Aag DNA glycosylase promotes alkylation-induced tissue damage mediated by Parp1. *PLoS Genet*. 2013;9:e1003413. <https://doi.org/10.1371/journal.pgen.1003413>.
- Ebrahimkhani MR, Mazumder A, Allocca M, et al. Aag-initiated base excision repair promotes ischemia reperfusion injury in liver, brain, and kidney. *Proc Natl Acad Sci USA*. 2014;111:E4878–E4886. <https://doi.org/10.1073/pnas.1413582111>.
- Winczura A, Zdzalik D, Tudek B. Damage of DNA and proteins by major lipid peroxidation products in genome stability. *Free Radical Res*. 2012;46:442–459. <https://doi.org/10.3109/10715762.2012.658516>.
- Chouchani ET, Pell VR, James AM, et al. A Unifying Mechanism for Mitochondrial Superoxide Production during Ischemia-Reperfusion Injury. *Cell Metab*. 2016;23:254–263. <https://doi.org/10.1016/j.cmet.2015.12.009>.
- Dixon M, Woodrick J, Gupta S, et al. Naturally occurring polyphenol, morin hydrate, inhibits enzymatic activity of N-methylpurine DNA glycosylase, a DNA repair enzyme with various roles in human disease. *Bioorg Med Chem*. 2015;23:1102–1111. <https://doi.org/10.1016/j.bmc.2014.12.067>.
- Mladěnka P, Zatloukalová L, Filipický T, Hrdina R. Cardiovascular effects of flavonoids are not caused only by direct antioxidant activity. *Free Radical Biol Med*. 2010;49:963–975. <https://doi.org/10.1016/j.freeradbiomed.2010.06.010>.
- Pietta P-G. Flavonoids as Antioxidants. *J Nat Prod*. 2000;63:1035–1042. <https://doi.org/10.1021/np9904509>.
- Carter AJ, Kraemer O, Zwick M, Mueller-Fahrnow A, Arrowsmith CH, Edwards AM. Target 2035: probing the human proteome. *Drug Discov Today*. 2019. <https://doi.org/10.1016/j.drudis.2019.06.020>.
- <https://www.thesgc.org/chemical-probes>.
- Lingaraju GM, Davis CA, Setser JW, Samson LD, Drennan CL. Structural basis for the inhibition of human alkyladenine DNA Glycosylase (AAG) by 3, N4-Ethenocytosine-containing DNA. *J Biol Chem*. 2011;286:13205–13213. <https://doi.org/10.1074/jbc.M110.192435>.
- Lau AY, Scharer OD, Samson L, Verdine GL, Ellenberger T. Crystal structure of a human alkylbase-DNA repair enzyme complexed to DNA: mechanisms for nucleotide flipping and base excision. *Cell*. 1998;95:249–258. [10](https://doi.org/10.1016/s0092-

</div>
<div data-bbox=)

- 8674(00)81755-9.
14. Schaerer OD, Ortholand J-Y, Ganesan A, Ezaz-Nikpay K, Verdine GL. Specific binding of the DNA repair enzyme AlkA to a pyrrolidine-based inhibitor. *J Am Chem Soc.* 1995;117:6623–6624. <https://doi.org/10.1021/ja00129a039>.
 15. Woods RD, O'Shea VL, Chu A, et al. Structure and stereochemistry of the base excision repair glycosylase MutY reveal a mechanism similar to retaining glycosidases. *Nucleic Acids Res.* 2015;44:801–810. <https://doi.org/10.1093/nar/gkv1469>.
 16. Schärer OD, Nash HM, Jiricny J, Laval J, Verdine GL. Specific binding of a designed pyrrolidine abasic site analog to multiple DNA glycosylases. *J Biol Chem.* 1998;273:8592–8597. <https://doi.org/10.1074/jbc.273.15.8592>.
 17. Deng L, Schärer OD, Verdine GL. Unusually strong binding of a designed transition-state analog to a base-excision DNA repair protein. *J Am Chem Soc.* 1997;119:7865–7866. <https://doi.org/10.1021/ja970828u>.
 18. Lau AY, Wyatt MD, Glassner BJ, Samson LD, Ellenberger T. Molecular basis for discriminating between normal and damaged bases by the human alkyladenine glycosylase. *AAG. Proc Natl Acad Sci.* 2000;97:13573–13578. <https://doi.org/10.1073/pnas.97.25.13573>.
 19. Schramm VL. Enzymatic transition states: thermodynamics, dynamics and analogue design. *Arch Biochem Biophys.* 2005;433:13–26. <https://doi.org/10.1016/j.abb.2004.08.035>.
 20. Singh V, Evans GB, Lenz DH, et al. Femtomolar transition state analogue inhibitors of 5'-methylthioadenosine/S-adenosylhomocysteine nucleosidase from *Escherichia coli*. *J Biol Chem.* 2005;280:18265–18273. <https://doi.org/10.1074/jbc.M414472200>.
 21. Hernández D, Boto A. Nucleoside analogues: synthesis and biological properties of azanucleoside derivatives. *Eur J Org Chem.* 2014;2014:2201–2220. <https://doi.org/10.1002/ejoc.201301731>.
 22. Miles RW, Tyler PC, Furneaux RH, Bagdassarian CK, Schramm VL. One-third-the-sites transition-state inhibitors for purine nucleoside phosphorylase. *Biochemistry.* 1998;37:8615–8621. <https://doi.org/10.1021/bi980658d>.
 23. Lewandowicz A, Tyler PC, Evans GB, Furneaux RH, Schramm VL. Achieving the ultimate physiological goal in transition state analogue inhibitors for purine nucleoside phosphorylase. *J Biol Chem.* 2003;278:31465–31468. <https://doi.org/10.1074/jbc.C300259200>.
 24. Lewandowicz A, Shi W, Evans GB, et al. Over-the-barrier transition state analogues and crystal structure with mycobacterium tuberculosis purine nucleoside phosphorylase. *Biochemistry.* 2003;42:6057–6066. <https://doi.org/10.1021/bi0343830>.
 25. Zhou G-C, Parikh SL, Tyler PC, et al. Inhibitors of ADP-ribosylating bacterial toxins based on oxocarbenium ion character at their transition states. *J Am Chem Soc.* 2004;126:5690–5698. <https://doi.org/10.1021/ja038159+>.
 26. Roday S, Amukele T, Evans GB, Tyler PC, Furneaux RH, Schramm VL. Inhibition of ricin A-chain with pyrrolidine mimics of the oxocarbenium ion transition state. *Biochemistry.* 2004;43:4923–4933. <https://doi.org/10.1021/bi0498499>.
 27. Jiang LY, Drohat AC, Ichikawa Y, Stivers JT. Probing the limits of electrostatic catalysis by uracil DNA glycosylase using transition state mimicry and mutagenesis. *J Biol Chem.* 2002;277:15385–15392. <https://doi.org/10.1074/jbc.M200634200>.
 28. Yuen PK, Green SA, Ashby J, et al. Targeting base excision repair glycosylases with DNA containing transition state mimics prepared via click chemistry. *ACS Chem Biol.* 2019;14:27–36. <https://doi.org/10.1021/acscchembio.8b00771>.
 29. Chu AM, Fetting JC, David SS. Profiling base excision repair glycosylases with synthesized transition state analogs. *Bioorg Med Chem Lett.* 2011;21:4969–4972. <https://doi.org/10.1016/j.bmcl.2011.05.085>.
 30. Zhang W, Rieger R, Iden C, Johnson F. Synthesis of 3, N4-etheno, 3, N4-ethano, and 3-(2-hydroxyethyl) derivatives of 2'-deoxycytidine and their incorporation into oligomeric DNA. *Chem Res Toxicol.* 1995;8:148–156. <https://doi.org/10.1021/tx00043a020>.
 31. Meier C, Jessen H. Lipophilic masked benzyl esters of nucleoside diphosphates and triphosphates as enzymatically hydrolyzable prodrugs for treatment of viral diseases, AIDS and cancers. Patent 2009 (WO2009129798A2): 49pp.
 32. Ladame S, Claustre S, Willson M. Selective phosphorylation on primary alcohols of unprotected polyols. *Phosphorus, Sulfur Silicon Relat Elem.* 2001;174:37–47. <https://doi.org/10.1080/10426500108040232>.
 33. Stowell JK, Widlanski TS. A new method for the phosphorylation of alcohols and phenols. *Tetrahedron Lett.* 1995;36:1825–1826. [https://doi.org/10.1016/0040-4039\(95\)00153-4](https://doi.org/10.1016/0040-4039(95)00153-4).
 34. Pradere U, Garnier-Amblard EC, Coats SJ, Amblard F, Schinazi RF. Synthesis of nucleoside phosphate and phosphonate prodrugs. *Chem Rev.* 2014;114:9154–9218. <https://doi.org/10.1021/cr5002035>.
 35. Filichev VV, Pedersen EB. Synthesis of 1'-aza-C-nucleosides from (3R,4R)-4-(hydroxymethyl)pyrrolidin-3-ol. *Tetrahedron.* 2001;57:9163–9168. [https://doi.org/10.1016/S0040-4020\(01\)00920-6](https://doi.org/10.1016/S0040-4020(01)00920-6).
 36. Filichev VV, Brandt M, Pedersen EB. Synthesis of an aza analogue of 2-deoxy-d-ribofuranose and its homologues. *Carbohydr Res.* 2001;333:115–122. [https://doi.org/10.1016/S0008-6215\(01\)00132-X](https://doi.org/10.1016/S0008-6215(01)00132-X).
 37. Evans GB, Cameron SA, Luxenburger A, et al. Tight binding enantiomers of pre-clinical drug candidates. *Bioorg Med Chem.* 2015;23:5326–5333. <https://doi.org/10.1016/j.bmc.2015.07.059>.
 38. Clinch K, Evans GB, Furneaux RH, et al. A practical synthesis of (3R,4R)-N-tert-butoxycarbonyl-4-hydroxymethylpyrrolidin-3-ol. *Org Biomol Chem.* 2007;5:2800–2802. <https://doi.org/10.1039/B708796A>.
 39. Kamath VP, Juarez-Brambila JJ, Morris CB, Winslow CD, Morris PE. Development of a practical synthesis of a purine nucleoside phosphorylase inhibitor: BCX-4208. *Org Process Res Dev.* 2009;13:928–932. <https://doi.org/10.1021/op9001142>.
 40. Karlsson S, Högberg H-E. Synthesis of enantiomerically pure 4-substituted pyrrolidin-3-ols via asymmetric 1,3-dipolar cycloaddition. *Tetrahedron Asymmetry.* 2001;12:1977–1982. [https://doi.org/10.1016/S0957-4166\(01\)00367-6](https://doi.org/10.1016/S0957-4166(01)00367-6).
 41. Kotian PL, Lin T-H, El-Kattan Y, Chand P. A practical large-scale synthesis of (3R,4R)-4-(Hydroxymethyl)pyrrolidin-3-ol via asymmetric 1,3-dipolar cycloaddition. *Org Process Res Dev.* 2005;9:193–197. <https://doi.org/10.1021/op049768k>.
 42. Clinch K, Evans GB, Fleet GWJ, et al. Syntheses and bio-activities of the L-enantiomers of two potent transition state analog inhibitors of purine nucleoside phosphorylases. *Org Biomol Chem.* 2006;4:1131–1139. <https://doi.org/10.1039/b517883e>.
 43. Allmendinger T, Bixel D, Clarke A, et al. Carry over of impurities: A detailed exemplification for glycopyrrolate (NVA237). *Org Process Res Dev.* 2012;16:1754–1769. <https://doi.org/10.1021/op3001788>.
 44. Roglans A, Marquet J, Moreno-Mañas M. Preparation of 3-pyrrolidone and 4-per-hydroazepinone. *Synth Commun.* 1992;22:1249–1258. <https://doi.org/10.1080/00397919208019306>.
 45. Pinto AC, Abdala RV, Costa PRR. Synthesis of chiral pyrrolidine and pyrrole derivatives through the chemoselective Dieckmann reaction of α , β -aminodiester. *Tetrahedron Asymmetry.* 2000;11:4239–4243. [https://doi.org/10.1016/S0957-4166\(00\)00377-3](https://doi.org/10.1016/S0957-4166(00)00377-3).
 46. Davis FA, Bowen KA, Xu H, Velvadapu V. Synthesis of polysubstituted pyrroles from sulfonimines (N-sulfinyl imines). *Tetrahedron.* 2008;64:4174–4182. <https://doi.org/10.1016/j.tet.2008.02.102>.
 47. Deshmukh MN, Gangakhedkar KK, Kumar US. Regioselective titanium tetrachloride mediated five membered hetero-cyclisations. *Synth Commun.* 1996;26:1657–1661. <https://doi.org/10.1080/00397919608002602>.
 48. Zhang T, Shen W, Liu M, et al. Synthesis, antimycobacterial and antibacterial activity of fluoroquinolone derivatives containing an 3-alkoxyimino-4-(cyclopropylamino) methylpyrrolidine moiety. *Eur J Med Chem.* 2015;104:73–85. <https://doi.org/10.1016/j.ejmech.2015.09.030>.
 49. Jaeger E, Biel JH. Pyrrolidinediols. 1-substituted 3-hydroxymethyl-4-hydroxypyrrolidines and derivatives. *J Org Chem.* 1965;30:740–744. <https://doi.org/10.1021/jo01014a019>.
 50. Jones K, Wilkinson J. A total synthesis of horsfiline via aryl radical cyclisation. *J Chem Soc, Chem Commun.* 1992;24:1767–1769. <https://doi.org/10.1039/C39920001767>.
 51. Macdonald TL, Narayanan BA. Pyrrolizidine alkaloid synthesis. (+)-Supinidine. *J Org Chem.* 1983;48:1129–1131. <https://doi.org/10.1021/jo00155a049>.
 52. Shim YK, Youn JI, Chun JS, Park TH, Kim MH, Kim WJ. A new synthesis of pyrroles. *Synthesis.* 1990;9:753–754. <https://doi.org/10.1055/s-1990-27004>.
 53. Galeazzi R, Martelli G, Mobbili G, Orena M, Rinaldi S. Chiral 3-hydroxypyrrolidin-2-ones from a Baylis-Hillman adduct: convergent, stereoselective synthesis of a glycosidase inhibitor. *Tetrahedron: Asymmetry.* 2004;15:3249–3256. <https://doi.org/10.1016/j.tetasy.2004.08.016> (Copyright (C) 2013 American Chemical Society (ACS). All Rights Reserved.).
 54. Basel Y, Hassner A. Di-tert-butyl dicarbonate and 4-(dimethylamino)pyridine revisited. Their reactions with amines and alcohols. *J Org Chem.* 2000;65:6368–6380. <https://doi.org/10.1021/jo000257f>.
 55. Bartoli G, Bosco M, Carlone A, et al. The first simple method of protection of hydroxy compounds as their O-boc derivatives under lewis acid catalysis. *Synlett.* 2006;2006:2104–2108. <https://doi.org/10.1055/s-2006-949609>.
 56. Singh SJ, Jayaram RV. Chemoselective O-tert-butoxycarbonylation of hydroxy compounds using NaLaTiO₄ as a heterogeneous and reusable catalyst. *Tetrahedron Lett.* 2008;49:4249–4251. <https://doi.org/10.1016/j.tetlet.2008.04.149>.
 57. Abdel-Magid AF, Carson KG, Harris BD, Maryanoff CA, Shah RD. Reductive amination of aldehydes and ketones with sodium triacetoxyborohydride. Studies on direct and indirect reductive amination procedures. *J Org Chem.* 1996;61:3849–3862. <https://doi.org/10.1021/jo960057x>.
 58. Goeminne A, Berg M, McNaughton M, et al. N-Arylmethyl substituted iminoribitol derivatives as inhibitors of a purine specific nucleoside hydrolase. *Bioorg Med Chem.* 2008;16:6752–6763. <https://doi.org/10.1016/j.bmc.2008.05.056>.
 59. Healing E, Charlier CF, Meira LB, Elliott RM. A panel of colorimetric assays to measure enzymatic activity in the base excision DNA repair pathway. *Nucleic Acids Res.* 2019;47:e61. <https://doi.org/10.1093/nar/gkz171>.
 60. Erlanson DA, Fesik SW, Hubbard RE, Jahnke W, Jhoti H. Twenty years on: the impact of fragments on drug discovery. *Nat Rev Drug Discovery.* 2016;15:605. <https://doi.org/10.1038/nrd.2016.109>.
 61. Hopkins AL, Keseru GM, Leeson PD, Rees DC, Reynolds CH. The role of ligand efficiency metrics in drug discovery. *Nat Rev Drug Discov.* 2014;13:105–121. <https://doi.org/10.1038/nrd4163>.
 62. Williams DBG, Lawton M. Drying of organic solvents: quantitative evaluation of the efficiency of several desiccants. *J Org Chem.* 2010;75:8351–8354. <https://doi.org/10.1021/jo101589h>.
 63. Li Z, Qian X, Xu Y. Synthesis and properties of oligonucleotides containing fluorescent ethenodeoxyadenosine and ethenodeoxycytidine. *Dyes Pigm.* 2002;54:247–252. [https://doi.org/10.1016/s0143-7208\(02\)00048-7](https://doi.org/10.1016/s0143-7208(02)00048-7).
 64. Wong U, Cox RJ. The chemical mechanism of D-1-deoxyxylulose-5-phosphate reductoisomerase from *Escherichia coli*. *Angew Chem Int Ed.* 2007;46:4926–4929. <https://doi.org/10.1002/anie.200700647>.
 65. Rosowsky A, Bader H, Forsch RA, Moran RG, Freisheim JH. Methotrexate analogs. 31. Meta and ortho isomers of aminopterin, compounds with a double bond in the side chain, and a novel analog modified at the α -carbon: chemical and in vitro biological studies. *J Med Chem.* 1983;31:763–768. <https://doi.org/10.1021/jm00399a013>.
 66. Momose T, Tanaka T, Yokota T. 4-Oxo-2-pyrrolines carrying no substituents on the ring carbon: substituent effects in the tautomerism between 4-oxo-2-pyrrolines and 3-hydroxypyrroles. *Heterocycles.* 1977;6:1827–1832. <https://doi.org/10.3987/R-1977-11-1827>.
 67. Evans GB, Furneaux RH, Lewandowicz A, Schramm VL, Tyler PC. Synthesis of second-generation transition state analogues of human purine nucleoside phosphorylase. *J Med Chem.* 2003;46:5271–5276. <https://doi.org/10.1021/jm030305z>.